SLAC-PUB-3799
CALT-68-1307
October 1985
(T/E)

New Results on Charmed D Meson Decay*

R.H. Schindler

California Institute of Technology
Pasadena, California 91125
and
Stanford Linear Accelerator Center
Stanford University, Stanford, California 94305

representing

The MARK III Collaboration

Abstract

In this paper we describe new measurements of D^0 and D^+ hadronic and semileptonic decays made with the MARK III detector at SPEAR. In the hadronic decays of the D^0 and D^+ , a high statistics determination of absolute D meson branching ratios is presented from fully reconstructed $D\bar{D}$ events. The same technique provides preliminary results of a search for $D^0\bar{D}^0$ mixing. Using the charm cross section established from fully reconstructed events we determine branching ratios for other newly observed Cabibbo allowed and suppressed hadronic decays. A detailed analysis of the Dalitz plot of 3-body D^0 and D^+ decays is presented. Measurements of hadronic decay processes leading to differences in D^0 and D^+ lifetimes are addressed. The semileptonic decays of charmed mesons are reviewed, and new exclusive measurements of the D_{e3} and D_{e4} decays are presented. The D_{e3} decays are used to extract for the first time the t-dependence of the vector form factor f_+ .

Invited talk presented at the SLAC Summer School on Physics of the
High Energy Accelerators, Stanford, California, July 15-26, 1985

* Work supported in part by the National Science Foundation and by the Department of Energy, contracts DE-AC03-76SF00515, DE-AC02-76ER01195, DE-AC03-81ER40050 and DE-AM03-76SF00034.

1. Introduction

The data reported on, ($9.25\ pb^{-1}$), were collected near the peak of the $\Psi(3770)$ resonance with the MARK III detector at SPEAR. The $\Psi(3770)$ provides a unique laboratory for studying charm meson decay. The measurements reported, rely on the unique kinematics of $D^0\bar{D}^0$ and D^+D^- production below $D\bar{D}^*$ threshold to isolate the charmed meson signal both cleanly and unambiguously. The ability to fully reconstruct $D\bar{D}$ events provides a means of directly measuring D meson branching ratios, makes possible a search for events where $D\bar{D}$ mixing occurs, and allows isolation for the first time of the D_{e3} and D_{e4} decays, wherein a single (unobserved) ν is present, Furthermore, the improvement obtained from kinematic constraints provides the background rejection necessary to measure rarer decays of the D^0 and D^+ .

The main thrust of our analysis has been in the understanding of the decay mechanisms of the charmed D, which lead to differences in D^0 and D^+ lifetimes.[1] In the naive Spectator Model, where the heavy c quark decays weakly, and the light quark plays no role, (see Figure 1 a), the D^0 and D^+ have equal widths. The semielectronic decays are 20% of the total. In the presence of strong interactions among the quarks, the nonleptonic decays are enhanced further over the semileptonic ones. These hard-gluon corrections to the weak Hamilitonian are calculable in perturbative QCD; the leading-log calculation indicates unambiguously that nonleptonic enhancement should be present.[2] The magnitude of the effect is however less certain, for the QCD coefficients (c_+ and c_-) depend both on the effective Q^2 of the interaction, the inclusion of higher order (next to leading -log) terms; the degree of color screening (ξ)

assumed (see Stech, ref. 1) is also critical. The higher order terms reinforce the direction toward nonleptonic enhancement, and are corrections of diminishing magnitude.[3] Semileptonic branching ratios obtained using nominal values for the QCD couplings are ~16%, reduced from 20% expected in the free quark picture; adjusting QCD parameters may lead to values as low as ~ 10%. Additional non-perturbative effects may be present, and play an important role further enhancing the nonleptonic widths,[4] and providing an *alternate* means of reducing the semileptonic branching ratios to as low as ~10%.

One sensitive test of these QCD calculations is their predictions of relative decay rates for hadronic channels. These calculations rely on factorization of the hadronic matrix element. Some decay modes such as $D^0 \rightarrow \bar{K}^0\pi^0$, *and* $\bar{K}^{*0}\pi^0$, *or* $D^+ \rightarrow \phi\pi^+$ may be subject to strong cancellations (*exact color suppression*) if naive color factors are applied (see ref. 2), and non-perturbative effects are unimportant. As nonleptonic QCD enhancement affects both D^0 and D^+ equally, it cannot by itself account for differences in lifetimes. One must look for ways of enhancing the D^0 or suppressing the D^+ to account for the observed differences. One mechanism proposed to enhance the D^0 is the inclusion of W-exchange graphs (see Figure 1(b)) in the amplitude. These will be present in the D^0 at the Cabibbo allowed level, and in the D^+ at the Cabibbo suppressed level. These graphs are generally ignored, being suppressed relative to spectator graphs by helicity factors at the light quark vertex ($(m_q/m_c)^2$), and by the requirement of a non-negligible wavefunction overlap ($(f_D/m_c)^2$). The combined effect would suppress the decays by 10^{-3} for values of f_D of a few hundred MeV. It is argued though, that either gluon radiation off the light quark,[5] or

simply the presence of color octet gluons in the D^0 wavefunction[6] could remove the helicity suppression and allow decays via W-exchange to proceed at a relative rate of order 10^{-1}. To test for the existence of the W-exchange graph requires finding decay channels which could proceed only through it and not the spectator. The requirement is thus a decay which has no u-quark in the final state, such as $D^0 \to \bar{K}^0\phi$, $\bar{K}^0K^0$, *or* $\bar{K}^{*0}K^0$. These decays should be dominated by W-exhange[7] with OZI forbidden contributions being down at the level of 10^{-4}.

An alternate solution to the lifetime puzzle is the possibility of destructive interference among D^+ decay amplitudes,[8] as shown in Figure 1(c). In the presence of strong color clustering during hadronization, the two amplitudes result in the same final state, allowing interference to occur. As in the case of W-exchange, the magnitude of the effect will depend on f_D, the overlap of quark wavefunctions at the origin. Such interference is possible in many 2-body D^+ decays such as $D^+ \to \bar{K}^0\pi^+$ *and* $\pi^+\pi^0$, but not in decays such as $D^+ \to \bar{K}^0K^+$ and $\bar{K}^{*0}K^+$.[9] This implies that a comparison of these channels may provide direct information on D^+ interference. The extent of the interference effect on the total width is uncertain.[10] What one should conclude from this brief discussion is that once convinced by the clean semileptonic decays or direct lifetime measurements that $\Gamma(D^+) \neq \Gamma(D^0)$, then understanding of the D decay mechanism(s) requires probing in detail the pattern of *hadronic* D decays.

In the following analyses, we rely on three of the major systems of the MARK III detector: the time-of-flight covering 76% of 4π sr with 190 ps resolution for hadrons, the central tracking chamber covering 85% of 4π sr, and the shower counters, covering 95% of 4π sr, having 100% detection efficiency for photons

over 0.1 GeV and having energy and space resolutions of 17% at 1 GeV, and 10mr respectively. The detector is described in detail elsewhere[11] .

2. The Measurement of Absolute Branching Ratios

The first measurment discussed is that of absolute branching ratios of hadronic decays. The general idea follows from the kinematics; if we can isolate a single charmed decay in an event, then we know *a priori* that the recoil system must also be a charmed meson, since only $D^0\bar{D}^0$ or D^+D^- are produced. The first step is to isolate background free samples of hadronic decays of D^0 and D^+ . In Figure 2 are shown the mass plots of D^0 and D^+ identified in six hadronic modes. There are 3435 D^0 and 1729 D^+ , where the excellent signal to background is achieved by imposing the constraint that the D's be produced monoenergetically. The next step, is to isolate the subset of events where the second D is also reconstructed. Six combinations of $D^0\bar{D}^0$ and four combinations of D^+D^- (see Figure 3) are employed. These events are referred to as *double tags*, while the first set are referred to as *single tags*, when the doubly tagged subset is removed. The numbers of events in each of these samples is simply related to the number of produced $D^0\bar{D}^0$ and D^+D^- events ($N_{D\bar{D}}$) and the branching ratios (B_i) for the i^{th} decay mode:

$$N_{D_i} = 2N_{D\bar{D}}\epsilon_i B_i \qquad \textit{single tags}$$

$$N_{D_iD_j} = 2N_{D\bar{D}}\epsilon_i B_i \epsilon_j B_j \qquad \textit{double tags}$$

where ϵ_i are the detection efficiencies determined by Monte Carlo calculation. A luminosity measurement is unnecessary. The system of equations is solved for D^0 and D^+ independently, with the results summarized in Table I-a and I-b.

Table I-a

Global Fit to D^0 Tags

	$K^-\pi^+$	$K^-\pi^+\pi^0$	$K^-\pi^+\pi^-\pi^+$
$K^+\pi^-$	26.0	95.3	49.9
(fit)	**25.7**	**90.6**	**57.8**
$K^+\pi^-\pi^0$		68.7	105.2
(fit)		**79.5**	**90.1**
$K^+\pi^-\pi^+\pi^-$			21.6
(fit)			**23.5**
single tags	936	1050	1049
(fit)	**931**	**1070**	**1043**

Table I-b

Global Fit to D^+ Tags

	$K^-\pi^+\pi^+$	$K^-\pi^+\pi^+\pi^0$	$K^0\pi^+$	$\bar{K}^0\pi^+\pi^0$
$K^+\pi^-\pi^-$	39.4	34.7	13.0	18.0
(fit)	**44.4**	**22.4**	**12.0**	**17.0**
single tags	1180	183	161	161
(fit)	**1172**	**215**	**163**	**164**

In Table II are presented the absolute branching ratios determined by this technique. In Table II are also included, decays not directly used in this analysis but whose branching ratio can now be obtained by global normalization to the number of produced D mesons from the fit.[12] Noteworthy among them are evidence for the 2-body decays $D^0 \to \bar{K}^0\eta$, and $D^0 \to \bar{K}^0\pi^0$, shown in Figure 4 . Also measured is the 2-body decay $D^0 \to \bar{K}^0\omega$. It is extracted from the $\bar{K}^0\pi^+\pi^-\pi^0$ by cuts on the $\pi^+\pi^-\pi^0$ invariant mass around the ω and in the ω sidebands to estimate background. This procedure is outlined in Figure 5 .

Table II

Cabibbo Allowed D^0 and D^+ Branching Ratios

Decay Mode	$\sigma \cdot Br$ (nb)	Br_{global} (%)	Br_{fit} (%)
$K^+\pi^-$	.237±.009±.013	4.9±0.4±0.4	5.1±0.4±0.4
$\bar{K}^0\pi^0$	.108±.020±.010	2.2±0.4±0.2	
$\bar{K}^0\eta$	.088±.039±012	1.8±0.8±0.3	
$\bar{K}^0\omega$	.187±.073±.047	3.8±1.5±1.0	
$K^-\pi^+\pi^0$	.978±.065±.137	20.1±1.9±3.0	18.5±1.3±1.6
$\bar{K}^0\pi^+\pi^-$	.372±.030±.031	7.6±0.8±0.7	
$K^-\pi^+\pi^-\pi^+$	.566±.027±.061	11.6±1.0±1.4	11.5±0.8±0.8
$\bar{K}^0\pi^+\pi^-\pi^0$	.666±.113±.153	13.7±2.5±3.2	
$\bar{K}^0\pi^+$	.126±.012±.009	3.5±0.5±0.4	4.0±0.6±0.4
$K^-\pi^+\pi^+$	.399±.017±.028	11.1±1.4±1.2	11.3±1.3±0.8
$\bar{K}^0\pi^+\pi^0$	.714±.142±.100	19.8±4.6±3.2	14.1±2.8±2.1
$\bar{K}^0\pi^+\pi^+\pi^-$	.305±.031±.030	8.5±1.3±1.1	
$K^-\pi^+\pi^+\pi^0$	.260±.040±.054	7.2±1.4±1.6	7.5±1.5±1.6

As can be seen from Table II, the branching ratios for the D^0 decays have typical errors of 10% while the D^+ decays have 15% errors. These generally are not arising from single tag statistics, but rather from double tags, which have a factor of $\epsilon_i \epsilon_j$ severely reducing the efficiencies. These rates then largely determine the error on the number of produced $D\bar{D}$ events: 22700±1600±1600 $D^0\bar{D}^0$ and 16800±2000±1600 D^+D^- . Dividing by the integrated luminosity (±5%), gives cross sections of $\sigma_{D^0} = 4.9 \pm 0.3 \pm 0.4$ nb and $\sigma_{D^+} = 3.6 \pm 0.4 \pm 0.4$ nb for D^0 and D^+ production at the $\Psi(3770)$. The ratio of cross sections (57:43) is consistent with the ratio expected (about 56:44) assuming phase space production and using the difference in D^0 and D^+ masses. The absolute cross sections are however considerably lower than previous experiments,[13] as indicated in Table III. The values of cross section times branching ratio ($\sigma \cdot Br$) for several prominent decay modes measured both by MARK III and by previous experiments are however in good agreement (see Table IV).[14]

Table III

Comparison of Cross Sections (nb) at the $\Psi(3770)$

	LGW	MARK II	C.B.	MARK III
σ_{D^0}	11.5±2.5	8.0±1.0±1.2	6.8±1.2	4.9±0.3±0.4
σ_{D^+}	9.0±2.0	6.0±0.7±1.0	6.0±1.1	3.6±0.4±0.4

Table IV

Comparison of $\sigma \cdot Br(nb)$ Among Experiments

Mode	LGW	MARK II	MARK III
$K^-\pi^+$	0.25±0.05	0.24±0.02	0.24±0.01±0.01
$K^-\pi^+\pi^+\pi^-$	0.36±0.10	0.68±0.11	0.57±0.03±0.06
$\bar{K}^0\pi^+$	0.14±0.05	0.14±0.03	0.13±0.01±0.01
$K^-\pi^+\pi^+$	0.36±0.06	0.38±0.05	0.40±0.02±0.03

This leads to the conclusion that discrepancies in early measurments of Br's lie largely with the normalization, which was previously determined indirectly by a measurement of the hadronic cross section around the $\Psi(3770)$. That measurement technique has distinct disadvantages, having uncertainties in lineshape, background from the Ψ' radiative tail, radiative corrections to the resonance itself, the division of phase space between $D^0\bar{D}^0$ and D^+D^- , and luminosity measurement.

3. The 3-Body Decays of D^0 and D^+

In the previous section, 3 and 4-body decays have been treated as they are *observed* in a particular final state. While no attempt has been made to isolate the substructure of 4-body decays (except $D^0 \rightarrow \bar{K}^0\omega$ via the $K^0\pi^+\pi^-\pi^0$ final state), an extensive Dalitz plot analysis has been performed to isolate the resonant substructure of the 3-body decays $D^0 \rightarrow \bar{K}^0\pi^+\pi^-, K^-\pi^+\pi^0$ and $D^+ \rightarrow \bar{K}^0\pi^+\pi^0$. The analysis of the fourth decay $D^+ \rightarrow K^-\pi^+\pi^+$ is not yet complete. The Dalitz plots and projections of each of these decays with the

two dimensional likelihood fit are shown in Figure 6 , Figure 7 and Figure 8 . The likelihood function is constructed as a sum of interfering Breit Wigner amplitudes for all allowed resonances, and a constant amplitude for the non-resonant part. Appropriate phase space factors and angular distributions are included for the pseudoscalar-vector channels. The background shape is scaled and smoothed from off-mass events. Efficiency corrections determined by Monte Carlo, are applied at each point of the Dalitz plot. Table V summarizes the fractional breakdown of the decays. The branching ratios for $K^-\pi^+\pi^0$ and $K^0\pi^+\pi^0$ come directly from the double-tag fit, while the $K^0\pi^+\pi^-$ uses the global fit. The $K^{*-}\pi^+$ decay provides a good check of systematics, as it is measured in both the $K^-\pi^+\pi^0$ and the $\bar{K}^0\pi^+\pi^-$ final states. As can be seen in Table V, both results are in excellent aggreement. after adjusting for Clebsch-Gordon coefficients. Table V shows that the class of quasi 2-body decays constitute a significant fraction of all hadronic D^0 and D^+ decays. From Table II and V we extract the following ratios, removing any common systematic errors:

$$\Gamma(D^0 \to \bar{K}^0\pi^0)/\Gamma(D^0 \to K^-\pi^+) = 0.45 \pm 0.08 \pm 0.05$$

$$\Gamma(D^0 \to \bar{K}^{*0}\pi^0)/\Gamma(D^0 \to K^{*-}\pi^+) = 0.30 \pm 0.14 \pm 0.08$$

$$\Gamma(D^0 \to \bar{K}^0\rho^0)/\Gamma(D^0 \to K^-\rho^+) = 0.09 \pm 0.03 \pm 0.02$$

Table V

Pseudoscalar-Vector Decays of D^0 and D^+

Decay Mode	Fraction (%)	$\sigma \cdot Br$ (nanobarns)	Br (%)
$D^0 \to K^-\pi^+\pi^0$			
$K^-\rho^+$	74.0±6.9	.72±.07±.11	13.7±1.3±1.5
$K^{*-}\pi^+$	12.9±3.4	.38±.09±.08	7.1 ±1.6±1.3
$\bar{K}^{*0}\pi^0$	7.6±3.9	.12±.05±.03	2.1 ±0.9±0.6
$non-resonant$	5.5±5.3	.05±.04±.03	1.0 ±0.8±0.6
$D^0 \to \bar{K}^0\pi^+\pi^-$			
$K^{*-}\pi^+$	63.9±8.8	.36±.05±.04	7.3±1.2±0.9
$\bar{K}^0\rho^0$	16.8±5.9	.06±.02±.01	1.3±0.4±0.3
$non-resonant$	19.3±9.3	.07±.03±.02	1.5±0.7±0.3
$D^+ \to \bar{K}^0\pi^+\pi^0$			
$\bar{K}^0\rho^+$	86.5±10.4	.62±.14±.09	12.2±2.8±1.9
$\bar{K}^{*0}\pi^+$	7.0±5.9	.15±.09±.09	3.0±1.9±1.7
$non-resonant$	6.5±6.8	.04±.04±.03	0.9±0.8±0.6

We pointed out earlier that these three decays provide a means of testing QCD parameters. The naive parameters (ref.2) predicted exact color suppression, which would lead to ratios of a *few percent* in each case. That they are not, suggests the need to fit these parameters (c_+, c_-, ξ), and account for final state interactions, and the possible presence of W-exchange. Fitting, to some extent accounts for the the presence of non-perturbative effects, altering the color structure of the hadronic weak decay.

4. The Cabibbo Suppressed Hadronic Decays

Thus far, the discussion has centered around the Cabibbo allowed decays of the D. The Cabibbo suppressed D decays are more difficult to measure as they occur at a rate approximately $tan^2(\theta_c) = .055$ relative to the allowed decays. We have previously reported an extensive set of measurements on the Cabibbo suppressed decays involving all charged tracks.[15] For decays with a single π^0, an alternate approach was taken to reduce combinatorial background. We search only in the tracks recoiling off a tagged D in the single tag event sample previously described. This approach yields clear signals for the the rare decays $D^+ \to \pi^+\pi^0$, $D^0 \to \pi^-\pi^+\pi^0$ and $D^0 \to \pi^-\pi^+\pi^-\pi^+$, as shown in Figure 9 . In each case we observe a clean, background free signal at the correct masses. The nine events in the 3-body decay $D^0 \to \pi^-\pi^+\pi^0$ are consistent with arising from $D^0 \to \rho^0\pi^0$ from an examination of both the invariant mass of the $\pi^+\pi^-$ and the decay angular distribution. The results of the measurements are summarized in Table VI (where limits are at 90% CL) along with previously reported results, now normalized to the global fit for absolute branching ratios.

The Cabibbo suppressed decays shed new light on the mechanism of D decay. First we note that the decay $D^+ \to \phi\pi^+$ is also a decay which would naively be suppressed by color factors (ref.10). It appears to occur at a substantial rate, as do other Cabibbo suppressed D^+ decays. Thus, exact color suppression appears inoperative in the D^+ as well as the D^0 system. Some of the suppression is lifted by adjusting QCD factors (ref.8), but non-perturbative effects or the presence of W-exchange may also provide a *common* explanation.

Table VI

Cabibbo Suppressed D^0 and D^+ Branching Ratios

Decay Mode	Br (%)
D^0	
K^-K^+	$0.60\pm0.10\pm.08$
$\pi^-\pi^+$	$0.16\pm0.05\pm.03$
$\bar{K}^0K^0$	≤ 0.62
$(K^0K^-\pi^+)_{nonres}$	≤ 1.80
$\bar{K}^0K^{*0}$	≤ 0.83
$K^{*-}K^+$	$1.02\pm0.47\pm0.21$
$\pi^-\pi^+\pi^0$	$1.11^{+0.43+0.18}_{-0.35-0.18}$
$\pi^-\pi^+\pi^-\pi^+$	$1.47^{+0.61+0.19}_{-0.49-0.19}$
D^+	
$\pi^+\pi^0$	≤ 0.53
$K^+\bar{K}^0$	$1.11\pm0.34\pm0.21$
$\pi^+\pi^+\pi^-$	$0.47\pm0.19\pm0.12$
$\phi\pi^+$	$0.93\pm0.26\pm0.17$
$\bar{K}^{*0}K^+$	$0.53\pm0.24\pm0.14$
$(K^-K^+\pi^+)_{nonres}$	$0.66\pm0.30\pm0.12$

We note from Table VI that the $\pi^+\pi^-$ and K^+K^- decays are unequal; a result which violates SU(3) symmetry.[16] The origin of the discrepancy is likely to be final-state interactions rather than differences in the mixing-matrix elements (in light of the recent measurements of the long B lifetime[17]). If we use these decays to set the scale of SU(3) violations then it is interesting to look at the analogous D^+ decays. SU(3) predicts that the decay $D^+ \rightarrow \pi^+\pi^0$ should have a

rate relative to $\bar{K}^0\pi^+$ of $1/2 \times tan^2(\theta_c)$ or about .028. In our sample we observe 141 $\bar{K}^0\pi^+$, and given the relative acceptance, we would expect to see 1.3 $\pi^+\pi^0$ events. We observe one event, and base our limit in Table VI on fluctuating that one event to 4.2 at 90% CL (including systematic error):

$$\Gamma(D^+ \to \pi^+\pi^0)/\Gamma(D^+ \to \bar{K}^0\pi^+) \leq 0.15$$

The analogous decay $D^+ \to \bar{K}^0K^+$ has no simple SU(3) prediction, as it brings in a third amplitude; however if it is comparable to the other amplitudes[18] then the ratio:

$$\Gamma(D^+ \to \bar{K}^0K^+)/\Gamma(D^+ \to \bar{K}^0\pi^+) = 0.32 \pm 0.09 \pm 0.05$$

should be close to $tan^2(\theta_c)$. As can be seen, the decay is considerably larger than that and considerably larger than what we would expect for SU(3) breaking effects, as measured in the D^0 system. This discrepancy may provide the first evidence for D^+ interference. Both $\pi^+\pi^0$ and $\bar{K}^0\pi^+$ are subject to such interference, while $\bar{K}^0K^+$ is not. This leaves the first ratio *normal*, while increasing the second substantially. Other evidence that exists is the similar comparison with $\bar{K}^{*0}K^+$ and $\bar{K}^{*0}\pi^+$. This ratio is poorly determined because of low statistics, but at $0.18 \pm 0.14 \pm 0.11$, it is intriguingly large as well. Finally, the fact that many D^+ Cabibbo suppressed decays appear large relative to corresponding Cabibbo allowed decays suggest that interference may be reducing the Cabibbo allowed sector. Several examples exist; $\bar{K}^0K^+$, $\bar{K}^{*0}K^+$, *and* $\phi\pi^+$ are seen to be large on average compared to the allowed decays $\bar{K}^0\pi^+$, *and* $\bar{K}^{*0}\pi^+$.[19]

5. The Non-Spectator Decays

The final topic on hadronic decays that I will discuss are the final states $D^0 \to \bar{K}^0 K^0$, $D^0 \to \bar{K}^{*0} K^0$ and $D^0 \to \bar{K}^0 \phi$. These are of particular theoretical interest because they may result only from the W-exchange graph in D^0 decay.

The $\bar{K}^0 K^0$ decay is Cabibbo suppressed as well as SU(3) forbidden, hence we expect its rate to be small. We observe one event consistent with the decay, and set the limit (see Figure 10):

$$\Gamma(D^0 \to \bar{K}^0 K^0)/\Gamma(D^0 \to K^- \pi^+) \leq 0.11 \; at \; 90\% \; CL$$

This upper limit is smaller than the analogous $K^- K^+$ decay.

The decays $D^0 \to \bar{K}^{*0} K^0$ *and* $\bar{K}^0 K^{*0}$ are not separable and are searched for in the final state $D^0 \to K^0_s K^{\pm} \pi^{\mp}$. The analysis proceeds by cutting on the mass of the K^* and the angular distribution of the K^* decay products in the D^0 rest frame. The results are shown in Figure 11 . The number of events are fitted, and the results unfolded using a the Monte Carlo to calculate the efficiencies both for loss, and for feedown across the channels. The results have already been summarized in Table VI, but for this discussion, we note that the ratio:

$$\Gamma(D^0 \to \bar{K}^{*0} K^0 + K^{*0} \bar{K}^0)/\Gamma(D^0 \to K^{*-} \pi^+ + K^- \rho^+) \leq 0.034 \; at \; 90\% \; CL$$

is small. While this is also a Cabibbo suppressed decay, it is not forbidden in SU(3).

This leads us to the last candidate, $\bar{K}^0 \phi$, a W-exchange signature which is Cabibbo allowed, and might appear at a level of .2 to .5 of the $K^0 \rho^0$ or .1 to

.2 of the $K^{*-}\pi^+$ rate, *if only* phase space and the suppression associated with $s\bar{s}$ production from the vacuum governs the rates.[20] The analysis proceeds as follows: K_s^0 are isolated through their $\pi^+\pi^-$ decay,where at least one of the π are required to miss the beam intersection point by more than 2mm. The pair, at their intersection point (the decay point of the K_s^0) must align within errors with the vector pointing back from the beam intersection. K_s^0 are selected by a mass cut $\pm 0.020 GeV/c^2$ around the expected mass. Charged kaons are selected by cuts on the time-of-flight, and because of the low Q value of this decay, DEDX information is also used. The 3-body combination is then formed and the invariant mass calculated. As any real D^0 are produced monoenergetically, we impose the constraint that the momentum of the 3-body combination lie within 0.050 GeV/c of the expected momentum. Off-momentum combinations from 0.060 to 0.110 GeV/c away from the expected value, are be used to estimate the shape of the background. The resulting mass distribution is shown in Figure 12 . There are 25.2 ± 5.4 events in the signal. The mass resolution is consistent with a Monte Carlo calculation. It should be noted that at this point in the analysis, we have made *no* requirements on the submasses K^-K^+ *or* $K^0K^\pm$. Figure 13 indicates that the K^+K^- mass will will not be distorted by detection efficiency near threshold. Furthermore, because of the kinematics, any reflections from particle misidentification in Cabibbo suppressed D^0 could *only* appear higher in mass by $\sim 0.110\ GeV/c^2$.

To study the question of submasses, we next select events from $\pm 0.040\ GeV/c^2$ around the D^0 mass. There are 28 such events, where we estimate 4.8 to be background. In Figure 14 (a) is plotted the mass distribution for the 28 K^-K^+ pairs

in the signal. If we define $1.019 \pm .015 GeV/c^2$ as the "ϕ region" (about 3.5σ of our ϕ resolution), then we find 4 events below, 11 events within, and 13 events above the ϕ region, respectively. Of these we expect 4.8 to be background. We have examined the various sources of background and their distribution which can feed into this plot:

1. The shape of K^+K^- mass distribution from the 4.8 random background events can be examined by looking at a sample of 25 off-momentum events (at the D^0 mass). In this sample, 5 events have a K^+K^- pair in the ϕ region. This yields a limit of ≤ 1.7 events, coming from this random background in the ϕ region.

2. Events from the Cabibbo suppressed decay $D^0 \rightarrow \phi\pi^+\pi^-$ will produce a peak at the ϕ. We have measured this decay directly (10.5 ± 5.5 events) by looking at $non - K^0$ combinations of $\pi^+\pi^-$. Because of the K^0_s vertex requirements, the contamination will be ≤ 0.3 events in the ϕ region.

3. Events from the Cabibbo suppressed decay $D^0 \rightarrow K^-K^+\pi^+\pi^-$ may contaminate the whole plot. We measure only an upper limit of 28 events. In the ϕ region we expect ≤ 0.14 events, while in whole Dalitz plot we expect ≤ 0.80 events, again because of the reduction from K^0_s vertex requirments.

4. Events from $D^0 \rightarrow K^0K^+K^-$ phase space if normalized to the events above the ϕ region, yield ≤ 0.70 events at the ϕ itself.

5. Events from $D^0 \rightarrow K^-\delta^+$ peak at high K^+K^- mass and if normalized to the events above the ϕ region, yield ≤ 0.20 events at the ϕ.

6. Events from $D^0 \rightarrow S^{*0}K^0$ would produce an S^* peak (cusp) below the ϕ.

The S^* decays as well to $\pi^+\pi^-$ [21] but is not seen in the $\bar{K}^0\pi^+\pi^-$ Dalitz plot (see Figure 7), we thus expect no contribution from this source.

7. This leaves us with the possible decay $D^0 \to K^0\delta^0$. This channel peaks at low K^+K^- mass and has a long tail.[22]

Figure 15 shows the Dalitz plots for the 28 data events and for 400 Monte Carlo events in each of the background channels discussed. The Monte Carlo events have been passed through the detector simulation and as such are directly comparable to the data in shape. Also included is a plot of the expected distribution for $\bar{K}^0\phi$, showing the strong angular distribution resulting from the pseudoscalar-vector decay. Neither the angular distribution nor a significant accumulation of events consistent with the ϕ are seen.

To be more quantitative, we have attempted to fit the K^+K^- projection of the Dalitz plot, to a sum of the ϕ, the δ^0 and a contribution which reflects the random background distribution in K^+K^-. For the background, the fit constrains the number of events to that measured (4.8 ± 2.4). The result is shown in Fig. 14(b). In the fit, 5.2 ± 3.3 events are assigned to ϕ hypothesis implying a branching ratio:

$$Br(D^0 \to \bar{K}^0\phi) = 0.7 \pm 0.5 \pm 0.2\%$$

Ignoring both the low mass events, and the high mass tail, we determine an upper limit of 2.5% at 90% CL, fitting only to the background and ϕ components (Fig. 14(c)).

If we interpret this as a signal, then in fact we would have to argue that the W-exchange graph is present, and *surprisingly large*. Our branching ratio of

about 0.7% makes it comparable to other pseudoscalar-vector decays like $\bar{K}^0\rho^0$ and $K^{*-}\pi^+$, if only phase space and the $(s\bar{s})$ suppression factor are accounted for, but no helicity or overlap suppression factors (ref. 20).

6. Search for $D^0\bar{D}^0$ Mixing

One other analysis employing fully reconstructed events, is a search for $D^0\bar{D}^0$ events exhibiting mixing. The signature would be events with two D^0 mesons having a net strangeness of ± 2 instead 0 in the final state. The analysis proceeds by fitting events with zero net charge to the hypothesis $e^+e^- \rightarrow \Psi(3770) \rightarrow X(M)\bar{X}(M)$ and plotting the mass M. X and $\bar{X}$ are allowed to decay to one of three possible modes: $K^\pm\pi^\mp, K^\pm\pi^\mp\pi^0$, *or* $K^\pm\pi^\mp\pi^\pm\pi^\mp$. Particle identification through time-of-flight and DEDX measurements has been tightened from the previous analysis, to reduce backgrounds from π and K misidentification. The kinematic fit also provides additional rejection, in particular from single misidentifications of Cabibbo forbidden decays which reconstruct off the D mass, but may be pulled by measurement error. In Figure 16 are shown the distributions of M_X for the six $\bar{X}X$ combinations. There are 162 S=0 events, and 3 S=$\pm$2 events. At this time, we have only evaluated the background to the $S = \pm 2$ events from double misidentifications of Cabibbo allowed decays. We expect from this source, 0.4 ± 0.2 events, based on a Monte Carlo calculation. This has been checked by relaxing the identification criteria and comparing the predicted and observed changes in the number of S=0 and S=$\pm$2 events. The systematic error so determined is expected to be less than 0.1 events and is included. The background estimate does *not* include other sources still under

consideration - such as those that lead to events observed below the D mass in the S=0 events. In the Standard Model, we expect doubly Cabibbo suppressed decays to occur at a rate of $tan^4(\theta_c)$ or about 3 x 10^{-3}. This implies that in the sample of 324 D^0 's, we would expect ~ 1 event from doubly suppressed decays of the D^0 . This leaves us with the intriguing result of 1.6 excess events, still far above the Standard Model estimate of 10^{-7} for the mixing fraction, corresponding to $\sim 3 \times 10^{-5}$ events expected in the sample.[23]

7. Inclusive Semileptonic Branching Ratios

Using the set of single tags described above, the semileptonic decays are isolated by finding events containing an electron in the recoiling system, with the expected charge based on the charm of the tag. This technique allows the unambiguous association of the electron with either a D^+ or D^0 decay, and hence the determination of separate semileptonic branching ratios. Electrons are identified from their time-of-flight, from their shower energy and momentum measurement, and from their lateral and longitudinal shower development in the fine-sampling electromagnetic calorimeter. The number of observed electrons is corrected for misidentification and efficiency, using rates measured from samples of independently isolated electrons and pions. The hadron misidentification rate is typically less than 4% while the electron efficiency is greater than 80%. The results for the corrected electron spectrum and the branching ratios have been

published.[24] The values determined are :

$$Br(D^0 \to e^+ + X) = 0.075 \pm 0.011 \pm 0.004$$

$$Br(D^+ \to e^+ + X) = 0.170 \pm 0.019 \pm 0.007$$

$$Br(D^+ \to e^+ + X)/Br(D^0 \to e^+ + X) = 2.3^{+0.5+0.1}_{-0.4-0.1}$$

From the likelihood function for the ratio, equality is ruled out at the 4.3σ level.

The inequality of semileptonic branching ratios reflects the difference in D^0 and D^+ lifetimes up to the difference in their respective Cabibbo suppressed semileptonic widths.[25] The value of the production weighted branching ratio for charm into electrons at the $\Psi(3770)$ is $11.7 \pm 1.00 \pm 0.50\%$ using the ratio (56:44). The inclusive average semileptonic branching ratio we obtain is close to that of MARK II,[26] ($10.0 \pm 3.2\%$) where the same absolute tagging technique was employed. It is however larger than other experiments ($8.0 \pm 1.5\%$ for DELCO[27] and $7.2 \pm 2.8\%$ for LGW[28]), which relied on charm cross section measurements for normalization. This provides further evidence that discrepancies in branching ratios stem largely from differences in charm cross section measurements.

8. The D_{e3} and D_{e4} Decays and a Measurement of the Vector Form Factor

A subset of the candidate inclusive semileptonic events can be *fully* reconstructed, having identified $K^\pm$ or K^0_s along with the electron, as well as possible additional $\pi^\pm$ and π^0. Because the 4-vector of the D is known *a priori* from the tag, the missing mass can be evaluated, and a set of exclusive decays containing

only a missing neutrino, isolated. Figure 17 shows the missing mass of the candidate events versus the mass of the tagging decay. Backgrounds are estimated from Monte Carlo, typically arising only in the D_{e3} decays, where π^0's can be lost, and $\pi^{\pm}$ misidentified as $e^{\pm}$. Events with a kaon and a pion along with the lepton are found to be dominently $K^*(892)$ as seen in Figure 18 ; the branching ratios are corrected accordingly and the results summarized in Table VII.

Table VII

Exclusive Semileptonic Branching Ratios

Channel	Events	Bkd. Events	Br(%)
$K^-e^+\nu$	49	2.4	3.2±0.5±0.1
$K^-\pi^0e^+\nu$	4	0.0	0.9±0.5±0.1
$\bar{K}^0\pi^-e^+\nu$	5	0.0	3.0±1.4±0.2
$K^{*-}e^+\nu$			3.9±1.5±0.2
$\bar{K}^0e^+\nu$	19	0.6	9.3±2.2±0.3
$K^-\pi^+e^+\nu$	21	0.0	4.1±0.9±0.1
$\bar{K}^{*0}e^+\nu$			6.2±1.4±0.4

The sum of the exclusive channels can be compared with the inclusive measurments; any differences would arise from Cabibbo suppressed semileptonic decays and possible higher multiplicity semileptonic decays (the inclusive results are shown in parenthesis):

$$Br(D^0 \to K^-e^+\nu + K^{*-}e^+\nu) = 7.1 \pm 1.6 \pm 0.2\% \qquad (7.5 \pm 1.2\%)$$

$$Br(D^+ \to K^0e^+\nu + \bar{K}^{*0}e^+\nu) = 15.5 \pm 2.6 \pm 0.4\% \qquad (17.0 \pm 2.0\%)$$

The differences are 5.3% and 8.8% of the total inclusive rate however the errors

do not allow us to be more quantitative.

The dynamics of the decay of the D^0 can be studied by measurements of the D_{e3} decays. The matrix element for $D^0 \rightarrow K^- e^+ \nu$ is given by a product of the V-A leptonic current (J^{lepton}) and the hadronic current:

$$M = G_f cos(\theta_c) f_+(t)(P_D + P_K)^\gamma J_\gamma^{lepton}$$

where P_D and P_K are the 4-momenta of the D and the K in the decay frame of the D, and $t = (P_D - P_K)^2$ is the momentum transfer squared, only a function of E_K. The form factor f_+ is associated with the vector part of the current as the D^0 and K^- are pseudoscalars. The analogous term in $f_-(t)$ vanishes relative to that of $f_+(t)$, like the square of the electron mass in the rate. Integrating over the lepton variables and the direction of the kaon, we obtain the kaon energy spectrum:

$$W_K \propto |f_+(t)|^2 (E_K^2 - m_K^2)^{3/2} \qquad (1)$$

In the rest frame of the D, W_K is *only* a function of E_K. The 49 events (with 2.4 background events contamination) of $D^0 \rightarrow K^- e^+ \nu$ can be used to extract $f_+(t)$. Having tagged the event, we can *uniquely* boost to the rest frame of the decaying D^0 and measure E_K, W_K and hence $f_+(t)$. The Dalitz plot (E_K *vrs* E_e) is shown in Figure 19 . The kaon detection efficiency is flat over most of the t range as shown in Figure 20 (a). The fall off at high t is associated with low momentum K^- ($\leq 200\ MeV/c$) which decay in the detector. Once a parametrization for the form factor is chosen, we can correct for efficiency and use (1) to fit for $f_+(t)$. The simplest form of $f_+(t)$ is that of a simple pole, corresponding in this case to

the exchange of a vector particle (F^*) with the quantum numbers of charm and strangeness:[29]

$$f_+(t) = f_+(0)\ \frac{M_{F^*}^2}{M_{F^*}^2 - t}$$

The fit shown in Figure 21(b) shows excellent agreement with the form chosen for $f_+(t)$, suggesting that the single vector exchange is an adequate description of the physical process. The value we determine for M_{F^*} is $2.1^{+1.7}_{-0.4}\ GeV/c^2$, the central value being close to that measured ($\sim 2.11\ GeV/c^2$) for the F^*.[30]

9. Conclusions

We have presented numerous results in this paper. which I summarize here :

• The D^0 and D^+ lifetimes are not equal. This is evidenced by the semileptonic branching fractions and their ratio:

$$Br(D^0 \to e^+ + X) = 0.075 \pm 0.011 \pm 0.004$$

$$Br(D^+ \to e^+ + X) = 0.170 \pm 0.019 \pm 0.007$$

$$Br(D^+ \to e^+ + X)/Br(D^0 \to e^+ + X) = 2.3^{+0.5+0.1}_{-0.4-0.1}$$

• The D_{e3} decays, suggests that a simple pole representing a single exchanged vector meson (the F^*) provides an adequate description of the dynamics. This is essential for calculations of hadronic widths which assume factorization (see Stech ref. 1).

• Through absolute measurements of hadronic branching ratios using double tags, we have now established the proper (absolute) scale with which to measure and compare decays, and can account for ~80% of all decays.

• The hadronic decays of D^0 and D^+ are *largely* quasi 2-body. This makes a theoretical calculation of total widths a more plausible goal.

• Exact color suppression originally expected (ref.2) in D^0 and D^+ decays is absent. This is evidenced by the non-negligible relative contributions:

$$\Gamma(D^0 \to \bar{K}^0\pi^0)/\Gamma(D^0 \to K^-\pi^+) = 0.45 \pm 0.08 \pm 0.05$$

$$\Gamma(D^0 \to \bar{K}^{*0}\pi^0)/\Gamma(D^0 \to K^{*-}\pi^+) = 0.30 \pm 0.14 \pm 0.08$$

$$\Gamma(D^0 \to \bar{K}^0\rho^0)/\Gamma(D^0 \to K^-\rho^+) = 0.09 \pm 0.03 \pm 0.02$$

$$\Gamma(D^+ \to \phi\pi^+/\Gamma(D^+ \to K^-\pi^+\pi^+) = 0.09 \pm 0.02 \pm 0.01$$

Recent work (see ref. 8) suggests that the level of color suppression should be treated as a parameter (ξ) along with the usual two QCD coefficients (c_+ and c_-), which specify hard-gluon effects. It is then possible to fit for a common set of parameters (notably $\xi = 0$, and the mass scale 1.5 GeV) and successfully reproduce these ratios, along with other hadronic widths. An alternate and successful fit leaves the screening parameter at its nominal value ($\xi = 1/3$) and evaluates the QCD coefficients at a lower mass scale $\sim$ 1 GeV, emphasizing the presence of non-perturbative effects. To distinguish these solutions requires further understanding of final state interactions, and the enhancement from W-exchange in both D^0 and D^+ decays.[31]

• There is evidence that interference plays a major role in D^+ decays explaining in part the difference in D^0 and D^+ lifetimes. Interference is indicated

by the ratios:

$$\Gamma(D^+ \to \pi^+\pi^0)/\Gamma(D^+ \to \bar{K}^0\pi^+) \leq 0.15$$

$$\Gamma(D^+ \to \bar{K}^0K^+)/\Gamma(D^+ \to \bar{K}^0\pi^+) = 0.32 \pm 0.09 \pm 0.05$$

$$\Gamma(D^+ \to \bar{K}^{*0}K^+)/\Gamma(D^+ \to \bar{K}^{*0}\pi^+) = 0.18 \pm 0.14 \pm 0.11$$

Interference may also be contributing to the relative size of Cabibbo allowed and forbidden D^+ absolute branching fractions. The suppressed decays $\bar{K}^0K^+$, $\bar{K}^{*0}K^+$, and $\phi\pi^+$ are seen to be large on average compared to the allowed decays $\bar{K}^0\pi^+$, *and* $\bar{K}^{*0}\pi^+$.

• There is weak evidence for the contribution of non-spectator diagrams (W-exchange) to the D widths:

$$\Gamma(D^0 \to \bar{K}^{*0}K^0)/\Gamma(D^0 \to K^-\pi^+) \leq 0.11 \text{ at } 90\%\ CL$$

$$\Gamma(D^0 \to \bar{K}^{*0}K^0 + K^{*0}\bar{K}^0)/\Gamma(D^0 \to K^{*-}\pi^+ + K^-\rho^+) \leq 0.034 \text{at } 90\%\ CL$$

$$Br(D^0 \to \bar{K}^0\phi) = 0.7 \pm 0.5 \pm 0.2\% \textit{ or } \leq 2.5\% \text{ at } 90\%\ CL$$

The ARGUS[32] and CLEO[33] groups have also presented evidence for the $\bar{K}^0\phi$ decay, with branching ratios of $1.4 \pm 0.4\%$ and 0.9 ± 0.6 *to* $1.3 \pm 0.6\%$ repectively, when normalized to our absolute branching ratios. Differences arise from the treatment of non-$\bar{K}^0\phi$ events in the data.

One plausible picture which emerges, and ties these measurements together looks as follows. Both D^0 and D^+ are subject to strong nonleptonic enhancement, further enhanced by non-perturbative effects. This enhancement arises naturally

from QCD. The magnitude can be adjusted by allowing the QCD factors to vary within a limited range. The semielectronic decays are suppressed as such from the 20% level of the free quark picture down below the purely perturbative value of $\sim 16\%$ to as low as $\sim 10\%$. The D^0 hadronic width is enhanced by W-exhange shortening its lifetime further, and reducing the semielectronic width down to the measured 7.5%. The D^+ hadronic width is suppressed by interference, lengthening its lifetime relative to D^0 , raising its semielectronic branching ratio up to the measured 17.0%, and in conjunction with W-annihilation, leaving its Cabibbo suppressed decays somewhat larger than naively expected. To quantify these arguments requires an additional theoretical understanding of the breakdown of perturbative QCD at these low Q^2, and additional measurements of decays which are sensitive to interference and W-exchange.

I would like to acknowledge I.Bigi for many useful and enthusiastic discussions concerning the interpretation of our data. This work was supported in part by the U.S. National Science Foundation and the U.S. Department of Energy under Contracts No.DE-AC03-76SF00515, No.DE-AC02-76ER01195, No.DE-AC03-81ER40050, and No.DE-AM03-76SF00034.

REFERENCES

1. For recent reviews see, L.-L.Chau, Phys.Rep. 95, 1, (1983),
   R. Rückl, Habilitationsschrift, Universität München (1983), and
   B.Stech, Heidelberg Preprint HD-THEP-85-8 (1985).
2. J.Ellis, M.K.Gaillard, D.V.Nanopoulos, Nucl.Phys. B100, 313 (1975).
   N.Cabibbo and L.Maiani, Phys.Lett. 73B, 418 (1978).
   B.Fakirov and B.Stech, Nucl. Phys. B133, 315 (1978).
3. G.Alterelli *et al.*, Phys.Lett. 99B, 141 (1981).
4. Y.Igarashi, S. Kitakado, M. Kuroda, Phys.Lett. 93B, 125 (1980).
   N. Deshpande,M. Gronau, and D. Sutherland, Phys.Lett. 90B, 431 (1980).
   M. Gronau, and D. Sutherland, Nucl.Phys. B183, 367 (1981).
5. M.Bander, D. Silverman, and A.Soni, Phys.Rev.Lett. 44, 7 (1980).
6. H. Fritzsch and P. Minkowski, Phys.Lett. 90B, 455 (1980).
7. I.I.Y.Bigi and M.Fukugita, Phys.Lett. 91B, 121 (1980).
8. B. Guberina *et al.*, Phys.Lett. 89B, 111 (1979).
   M.Bauer and B.Stech, Phys.Lett. 152B, 380 (1985).
   A.J.Buras, Preprint MPI-PAE/PTh 64/85 (1985).
9. I.I.Y.Bigi, Phys.Lett. 90B, 177, (1980).
10. See Rückl, ref. 1., and references therein .
    R.Rückl, in *Proc. of the Int. Conf.on High Energy Physics, Leipzig,E.Germany, (1984)*, Vol.1,p. 135.
11. D.Bernstein *et al.*, Nucl. Instrum. Methods 226, 301 (1984).

12. The 3-body decays in Table II have been corrected for efficiency using their measured resonant substructure (see section 3). The implementation of this correction accounts for a large part of the increase in $\sigma \cdot Br$ over previously reported values.

13. P.A.Rapidis *et al.*, Phys.Rev.Lett. 39, 526 (1977),
W.Bacino *et al.*, Phys.Rev.Lett. 40, 671 (1978),
R.H.Schindler *et al.*, Phys.Rev. D21, 2716 (1980),
H. Sadrozinski,XX^{th} Int. Conf. on High Energy Phys ics,Madison, Wisconsin (1980).

14. R.H.Schindler *et al.*, Phys.Rev., D24, 78 (1981),
I.Peruzzi *et al.*, Phys.Rev.Lett., 39, 1301 (1977).

15. R.M.Baltrusaitis *et al.*, Phys.Rev.Lett. 55, 150 (1985).

16. R.L.Kingsley *et al.*, Phys.Rev. D11, 1919 (1975).
M. Einhorn and C.Quigg, Phys.Rev. D12, 2015 (1975).

17. L.-L.Chau and W.-Y. Keung, Phys.Rev. D29, 592,(1984).

18. A comparison of the $\bar{K}^0 K^+$ decay with $D^0 \to K^- \pi^+$ using the relative D^0 and D^+ lifetimes implies that the third amplitude is only about 30% larger than the first and second.

19. I.I.Y. Bigi, Aachen Preprint 85-0629 (1985).

20. I.I.Y.Bigi and M.Fukugita, Phys.Lett. 91B, 121 (1980) .

21. G.Gidal *et al.*, Phys.Lett. 107B 153, (1981).

22. The form is suggested by S.M.Flatte, Phys.Lett. 63B,224 (1976).

23. L.L.Chau Phys.Rep. 95, 1 (1983).

24. R.M.Baltrusaitus *et al.*, Phys.Rev.Lett. 54,1976 (1985).

25. A. Pais and S.B.Treiman, Phys.Rev. D15, 2529 (1977).
U. Baur and H. Fritzsch, Phys.Lett. 109B, 402 (1982).

26. R.H.Schindler *et al.*, Phys. Rev. D24, 78 (1981).

27. W. Bacino *et al.*, Phys.Rev.Lett. 43, 1073 (1979).

28. J.M.Feller *et al.*, Phys.Rev.Lett. 40, 274 (1978).

29. J. M. Gaillard, M. K. Gaillard, F. Vannucci, Weak Interactions (Institut National de Physique Nucléaire et de Physique des Particules, Paris, 1977), p. 63. This form is valid for a *narrow* resonance even if its central mass is below threshold.

30. H.Aihara *et al.*, Phys.Rev.Lett. 53, 2465 (1984).
H.Albrecht *et al.*, Phys.Lett. 146B, 111 (1984).

31. Private communication, I.I.Y. Bigi.

32. H.Albrecht *et al.*, Phys.Lett. 158B, 525 (1985).

33. P.Avery *et al.*, submitted to the 1985 Lepton Photon Symposium, Kyoto, Japan.

FIGURE CAPTIONS

1. Possible decay mechanisms for heavy quarks.

2. D^0 and D^+ single tags.

3. The mass for events where both $D^0\bar{D}^0$ or
   D^+D^- are reconstructed in each topology indicated.

4. (a)$D^0 \to \bar{K}^0\eta$, and (b)$D^0 \to \bar{K}^0\pi^0$

5. (a)$K^0\pi^+\pi^-\pi^0$, (b)with $\pi^+\pi^-\pi^0$ in ω band,
   and (c)with $\pi^+\pi^-\pi^0$ in ω sideband.

6. (a) $D^0 \to K^-\pi^+\pi^0$ Dalitz plot, (b) $\pi^+\pi^0$ projection, (c) $K^-\pi^0$ projection,
   (d) $K^-\pi^+$ projection. The solid curve is the fit.

7. (a) $D^0 \to K^0\pi^+\pi^-$ Dalitz plot, (b) $\pi^+\pi^-$ projection, (c) $K^0\pi^+$ projection,
   (d) $K^0\pi^-$ projection. The solid curve is the fit.

8. (a) $D^+ \to K^0\pi^+\pi^0$ Dalitz plot,(b) $\pi^+\pi^0$ projection ,(c) $K^0\pi^+$ projection,
   (d) $K^0\pi^0$ projection. The solid curve is the fit.

9. Constrained mass for (a)$\pi^+\pi^0$, (b)$\pi^-\pi^+\pi^0$ and (c)$\pi^-\pi^+\pi^-\pi^+$.

10. $\bar{K}^0K^0$ invariant mass vrs constrained mass.

11. (a)$K^0K^-\pi^+ + \bar{K}^0K^+\pi^-$ (non-resonant),
    (b)$\bar{K}^{*0}K^0 + \bar{K}^0K^{*0}$, and
    (c)$K^{*-}K^+ + K^{*+}K^-$.

12. $K^0_sK^+K^-$ mass distribution and fit. The background is
    derived from off-momentum events.

13. Relative K^+K^- efficiency for decays
    of (a) pseudoscalar or (b) vector states.

14. (a)K^+K^- mass in $K_s^0K^+K^-$,(b)Fit including background,
    $\bar{K}^0\phi$, and $\bar{K}^0\delta^0$ and (c)Fit for upper limit assuming
    $\bar{K}^0\phi$ and background.

15. Dalitz plot for data, and Monte Carlo of possible backgrounds.

16. The mass distributions (M) for $\Psi(3770) \rightarrow X(M)\bar{X}(M) \rightarrow$S=0
    and S=$\pm$2 events.

17. Missing mass^2 versus tagged mass for each channel indicated.

18. K^* from D^+ and D^0 semileptonic channels.

19. Dalitz plot for $D^0 \rightarrow K^-e^+\nu$.

20. (a) $K^\pm$ detection efficiency in the D^0 rest frame.
    (b) Efficiency corrected kaon energy spectrum (E_K) and
    fit assuming the simple pole form for $f_+(t)$.

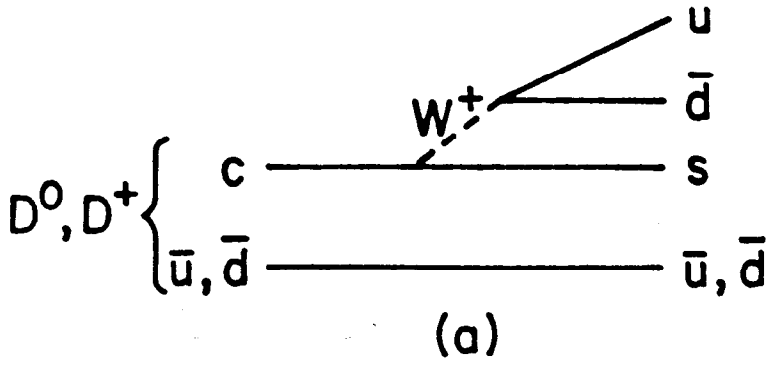
u
d̄
W+
c
s
D0, D+
ū, d̄
ū, d̄

(a)

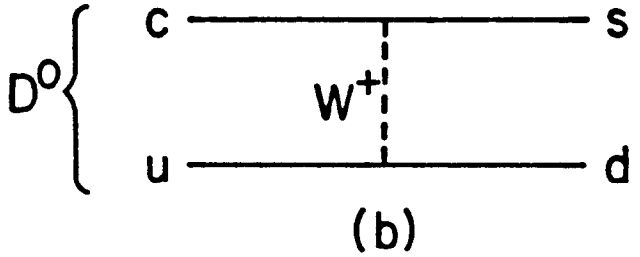
c
s
W+
D0
u
d

(b)

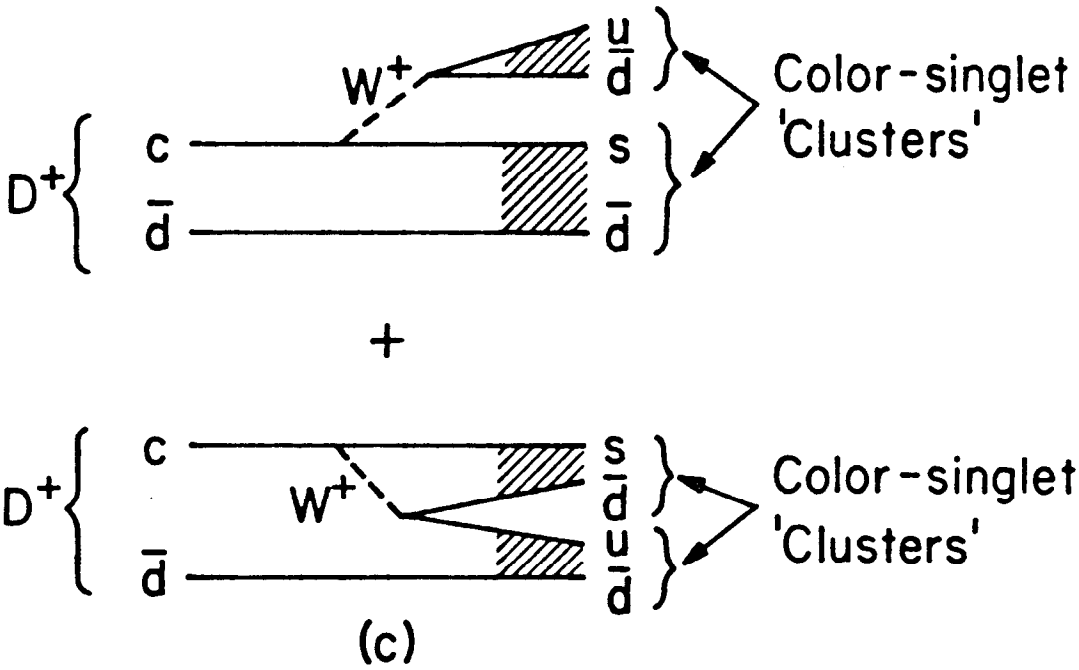
u
d̄
W+
Color-singlet
'Clusters'
c
s
D+
d̄
d̄
+
c
s
W+
d̄
D+
u
d̄
d̄
Color-singlet
'Clusters'

(c)

Fig. 1

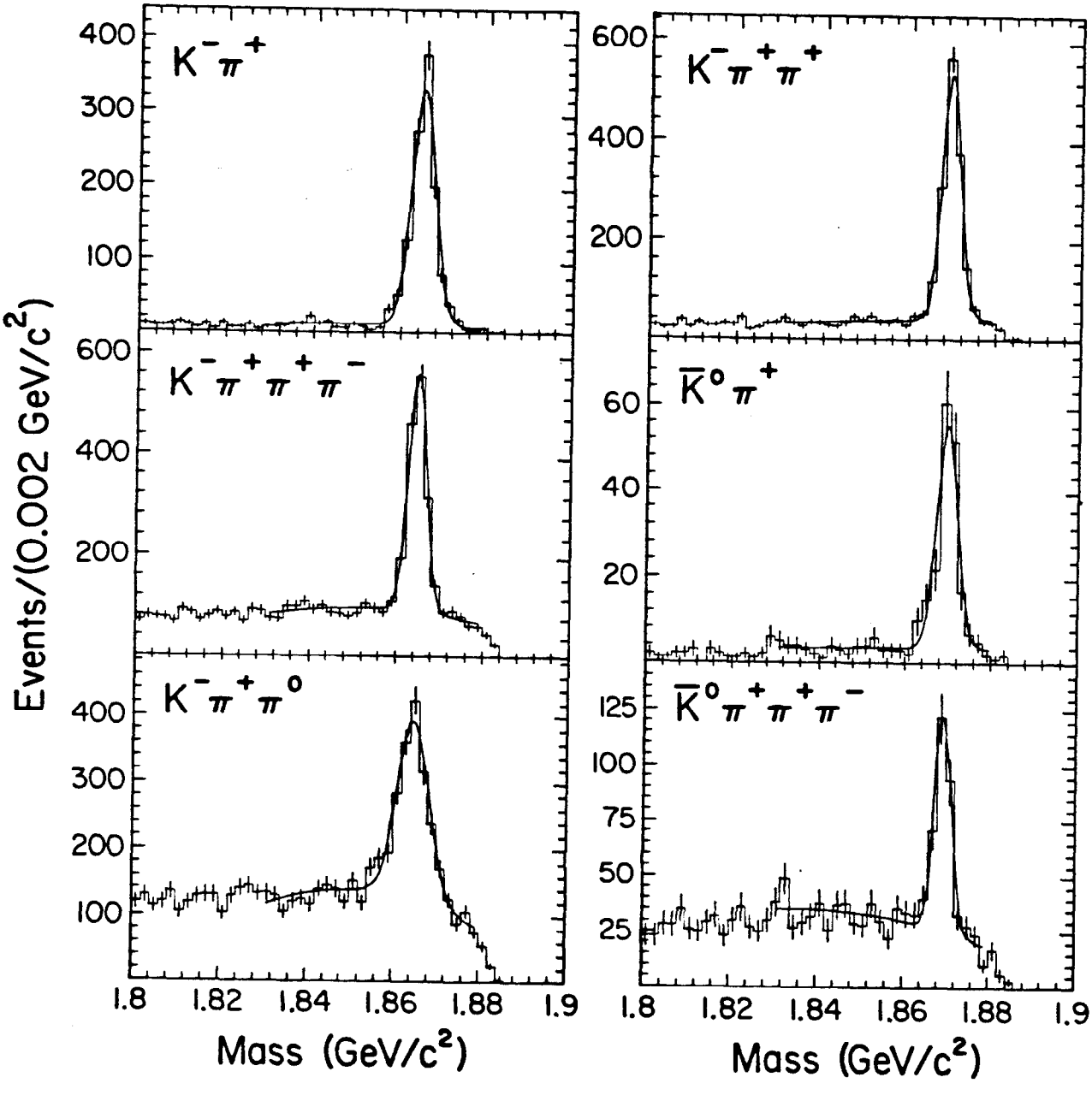
$K^-\pi^+$
$K^-\pi^+\pi^+$
$K^-\pi^+\pi^+\pi^-$
$\bar{K}^0\pi^+$
$K^-\pi^+\pi^0$
$\bar{K}^0\pi^+\pi^+\pi^-$
Events/(0.002 GeV/c^2)
Mass (GeV/c^2)
Mass (GeV/c^2)

Fig. 2

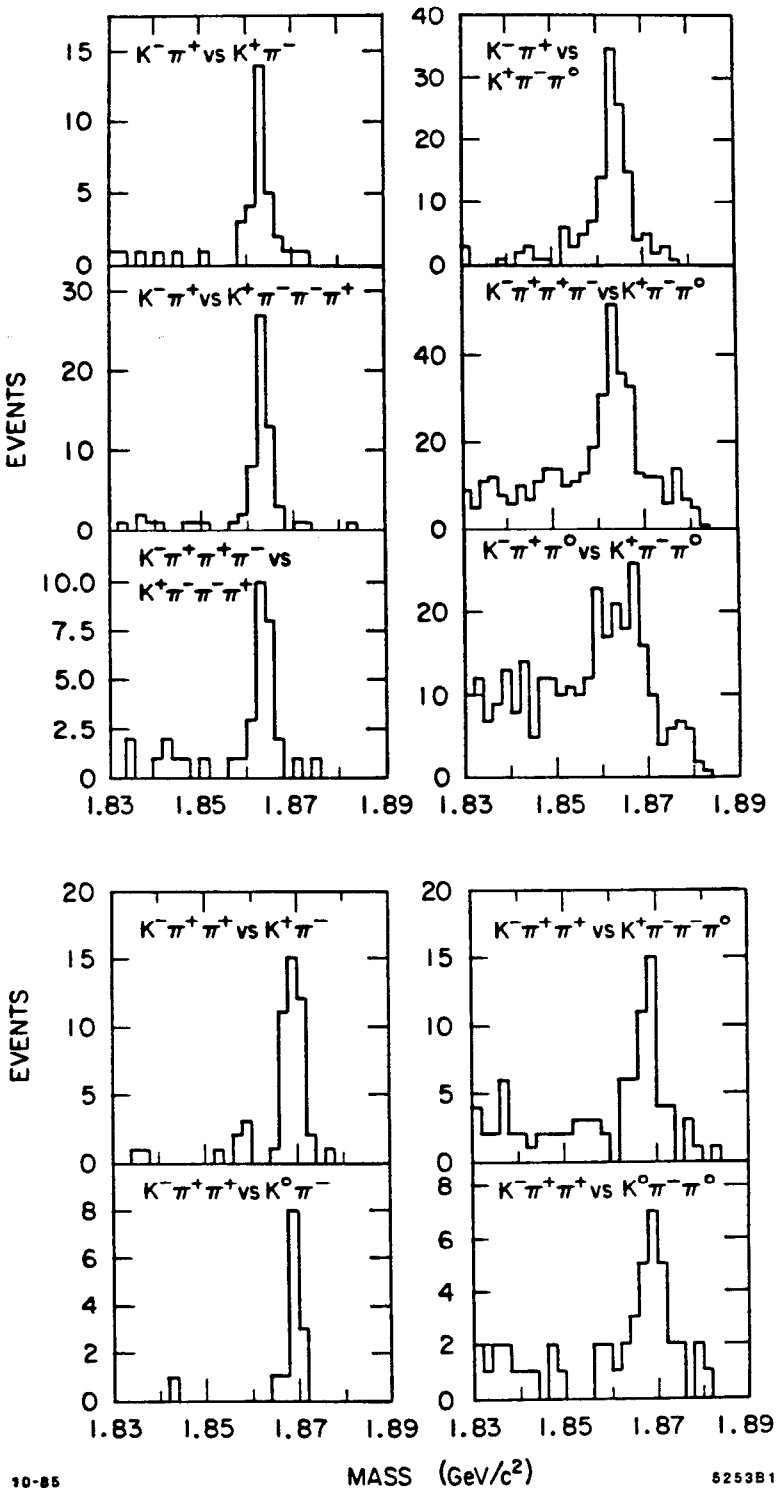
$K^-\pi^+$ vs $K^+\pi^-$
$K^-\pi^+$ vs $K^+\pi^-\pi^\circ$
$K^-\pi^+\pi^+\pi^-$ vs $K^+\pi^-\pi^-\pi^+$
$K^-\pi^+\pi^+\pi^-$ vs $K^+\pi^-\pi^\circ$
$K^-\pi^+\pi^+\pi^-$ vs $K^+\pi^-\pi^-\pi^+$
$K^-\pi^+\pi^\circ$ vs $K^+\pi^-\pi^\circ$
$K^-\pi^+\pi^+$ vs $K^+\pi^-$
$K^-\pi^+\pi^+$ vs $K^+\pi^-\pi^-\pi^\circ$
$K^-\pi^+\pi^+$ vs $K^\circ\pi^-$
$K^-\pi^+\pi^+$ vs $K^\circ\pi^-\pi^\circ$
EVENTS
EVENTS
MASS (GeV/c^2)
10-85
5253B1

Fig. 3

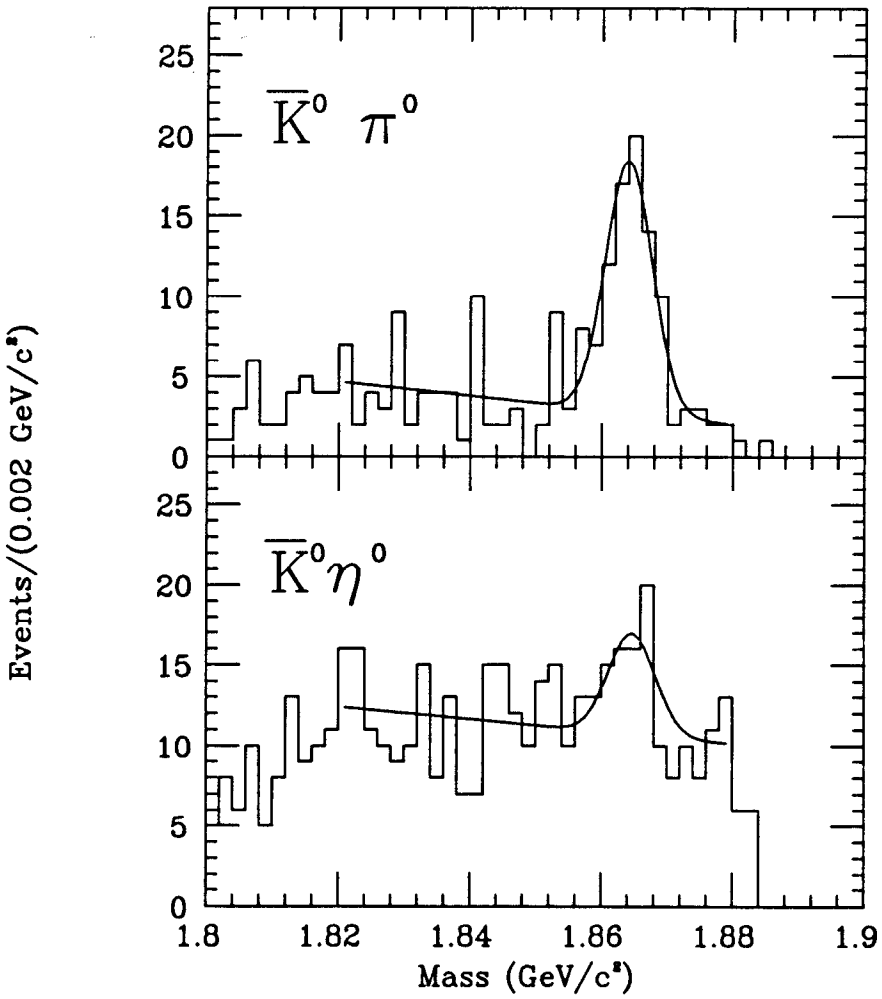
$\overline{K}^0\ \pi^0$
$\overline{K}^0\eta^0$
Events/(0.002 GeV/c²)
Mass (GeV/c²)
0
5
10
15
20
25
1.8
1.82
1.84
1.86
1.88
1.9

Fig. 4

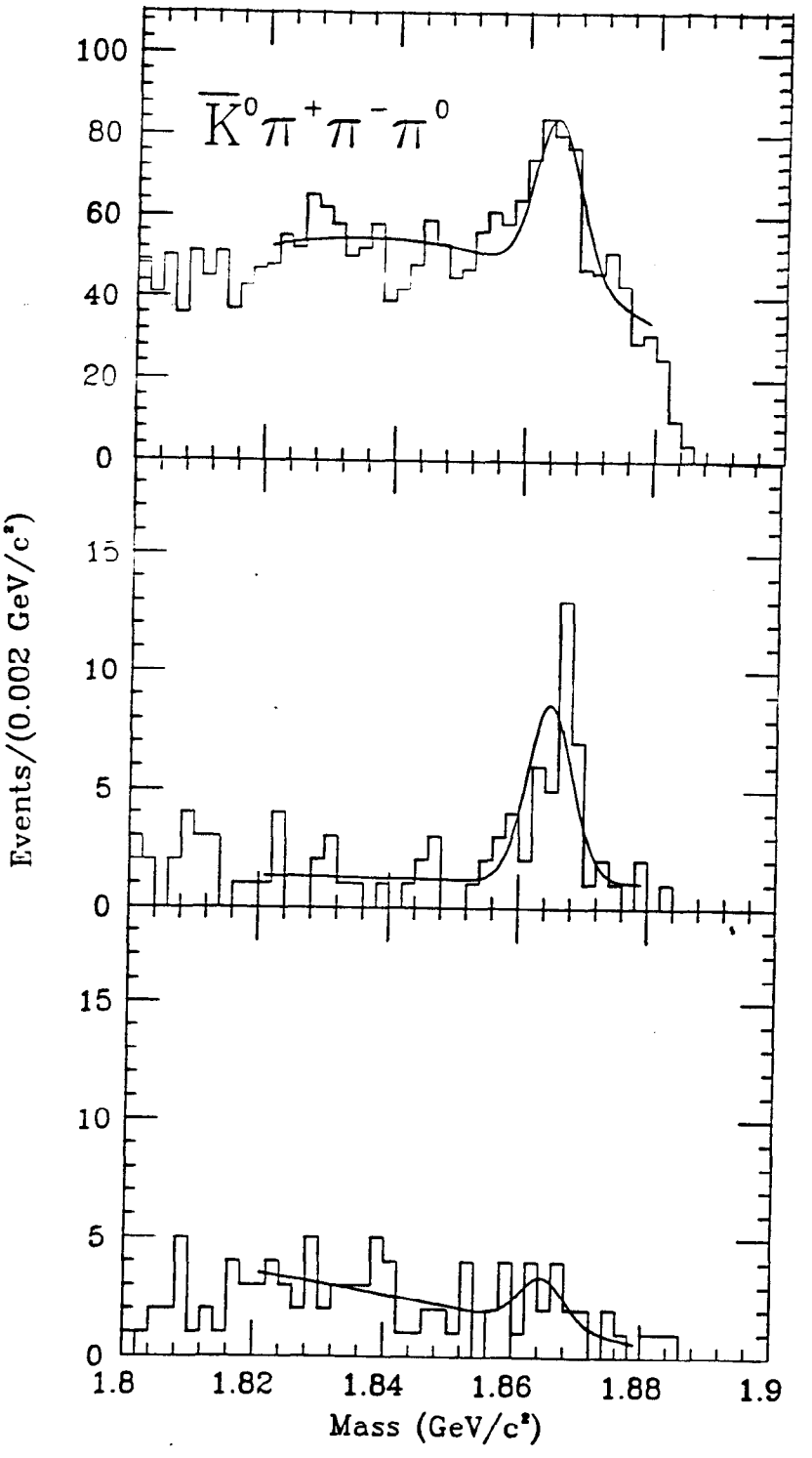
$\overline{K}^0\pi^+\pi^-\pi^0$
Events/(0.002 GeV/c²)
Mass (GeV/c²)
100
80
60
40
20
0
15
10
5
0
15
10
5
0
1.8
1.82
1.84
1.86
1.88
1.9

Fig. 5

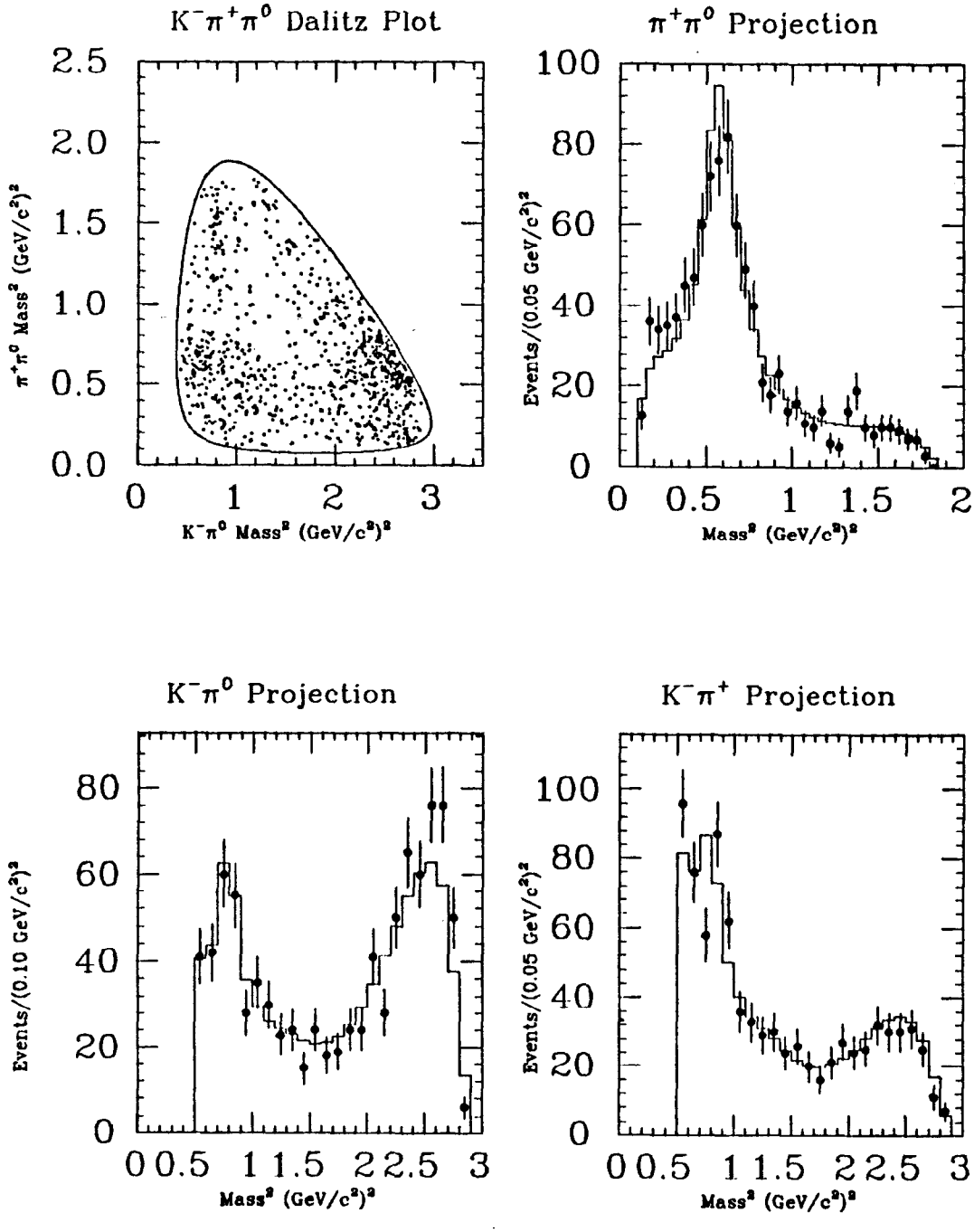
$K^-\pi^+\pi^0$ Dalitz Plot
$\pi^+\pi^0$ Mass^2 (GeV/c^2)^2
$K^-\pi^0$ Mass^2 (GeV/c^2)^2
$\pi^+\pi^0$ Projection
Events/(0.05 GeV/c^2)^2
Mass^2 (GeV/c^2)^2
$K^-\pi^0$ Projection
Events/(0.10 GeV/c^2)^2
Mass^2 (GeV/c^2)^2
$K^-\pi^+$ Projection
Events/(0.05 GeV/c^2)^2
Mass^2 (GeV/c^2)^2

Fig. 6

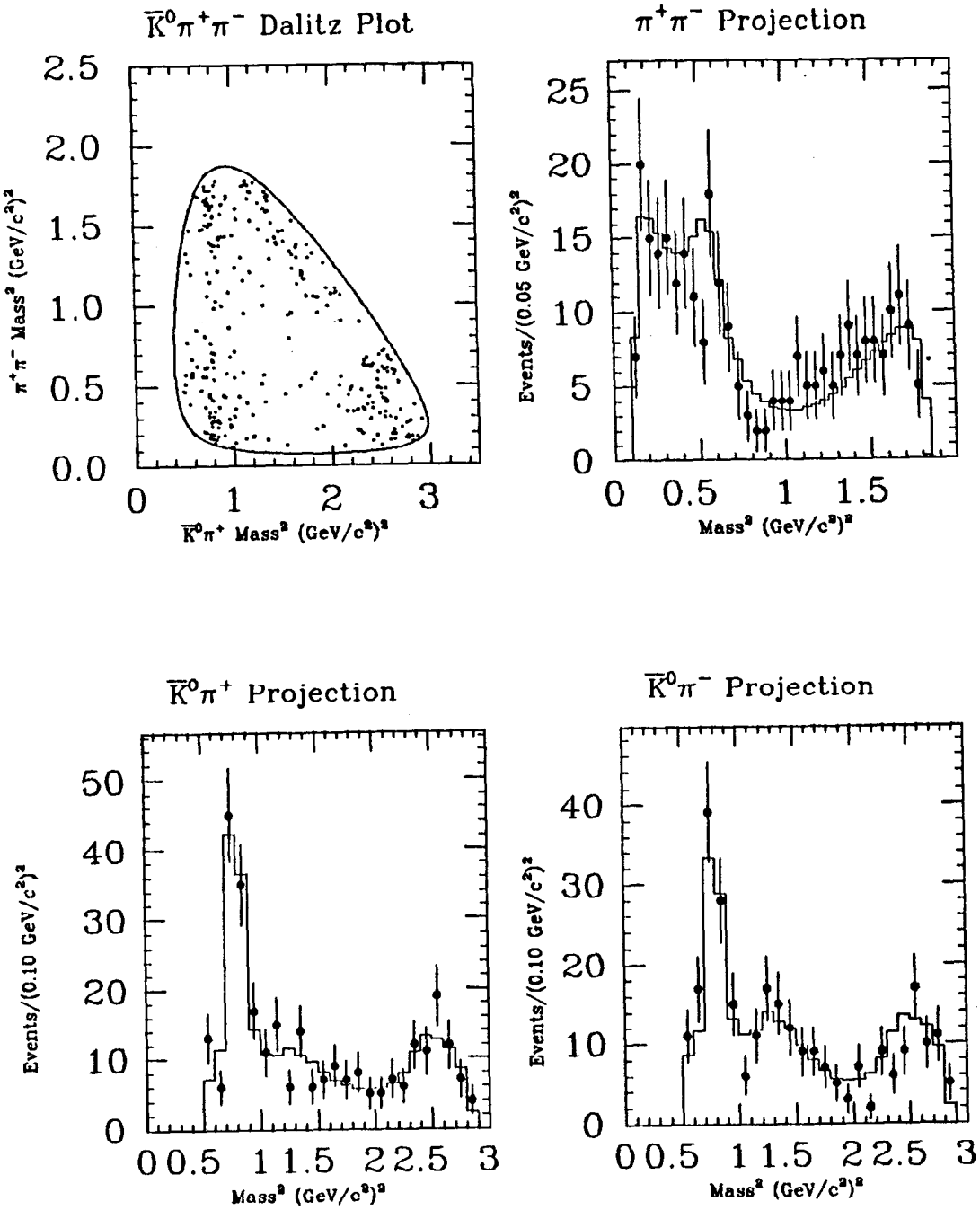
$\bar{K}^0\pi^+\pi^-$ Dalitz Plot
$\pi^+\pi^-$ Mass^2 (GeV/c^2)^2
$\bar{K}^0\pi^+$ Mass^2 (GeV/c^2)^2
$\pi^+\pi^-$ Projection
Events/(0.05 GeV/c^2)^2
Mass^2 (GeV/c^2)^2
$\bar{K}^0\pi^+$ Projection
Events/(0.10 GeV/c^2)^2
Mass^2 (GeV/c^2)^2
$\bar{K}^0\pi^-$ Projection
Events/(0.10 GeV/c^2)^2
Mass^2 (GeV/c^2)^2

Fig. 7

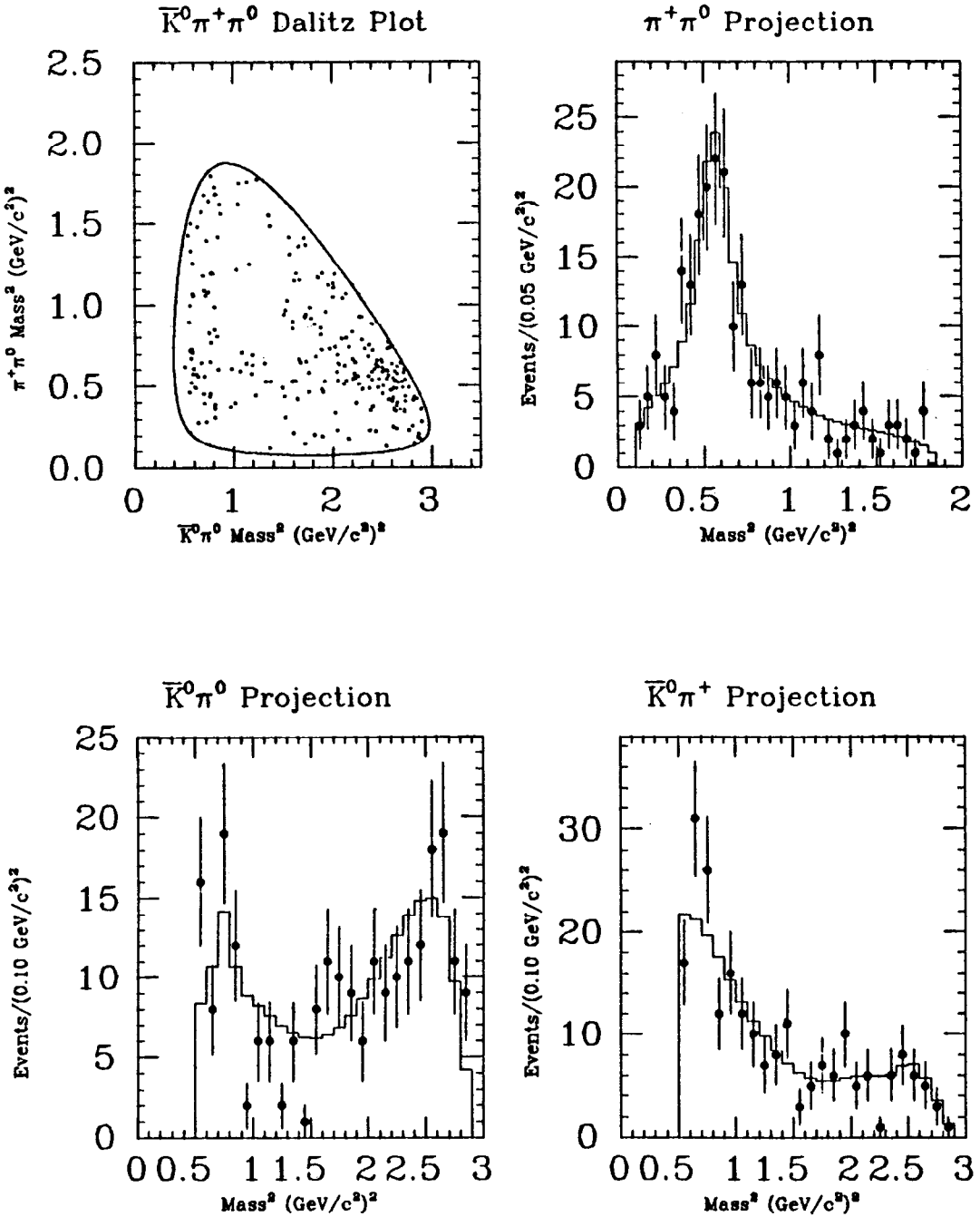
$\bar{K}^0\pi^+\pi^0$ Dalitz Plot
$\pi^+\pi^0$ Mass^2 (GeV/c^2)^2
$\bar{K}^0\pi^0$ Mass^2 (GeV/c^2)^2
$\pi^+\pi^0$ Projection
Events/(0.05 GeV/c^2)^2
Mass^2 (GeV/c^2)^2
$\bar{K}^0\pi^0$ Projection
Events/(0.10 GeV/c^2)^2
Mass^2 (GeV/c^2)^2
$\bar{K}^0\pi^+$ Projection
Events/(0.10 GeV/c^2)^2
Mass^2 (GeV/c^2)^2

Fig. 8

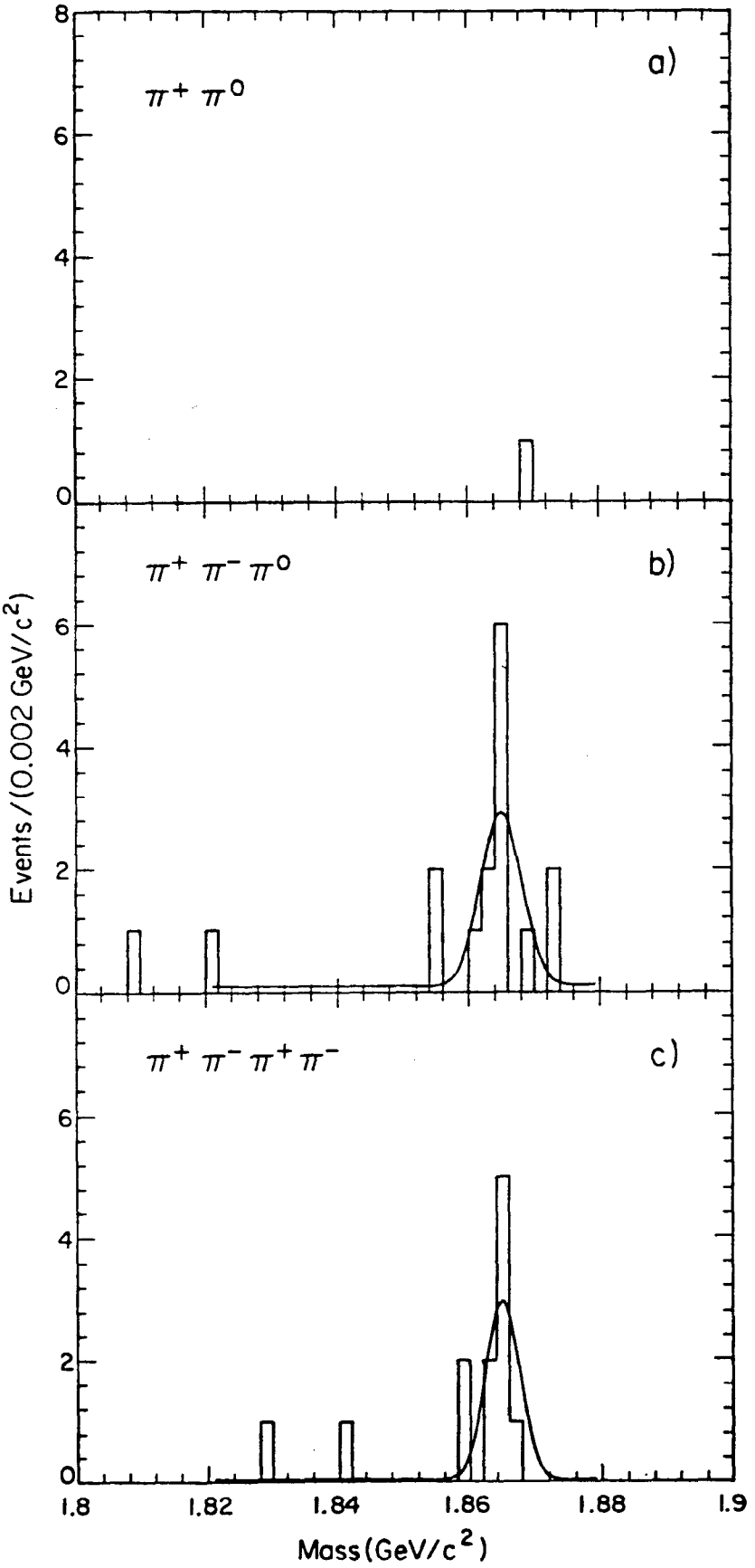
a)
$\pi^+ \pi^0$
b)
$\pi^+ \pi^- \pi^0$
c)
$\pi^+ \pi^- \pi^+ \pi^-$
Events/(0.002 GeV/c^2)
Mass(GeV/c^2)
0
2
4
6
8
1.8
1.82
1.84
1.86
1.88
1.9

Fig. 9

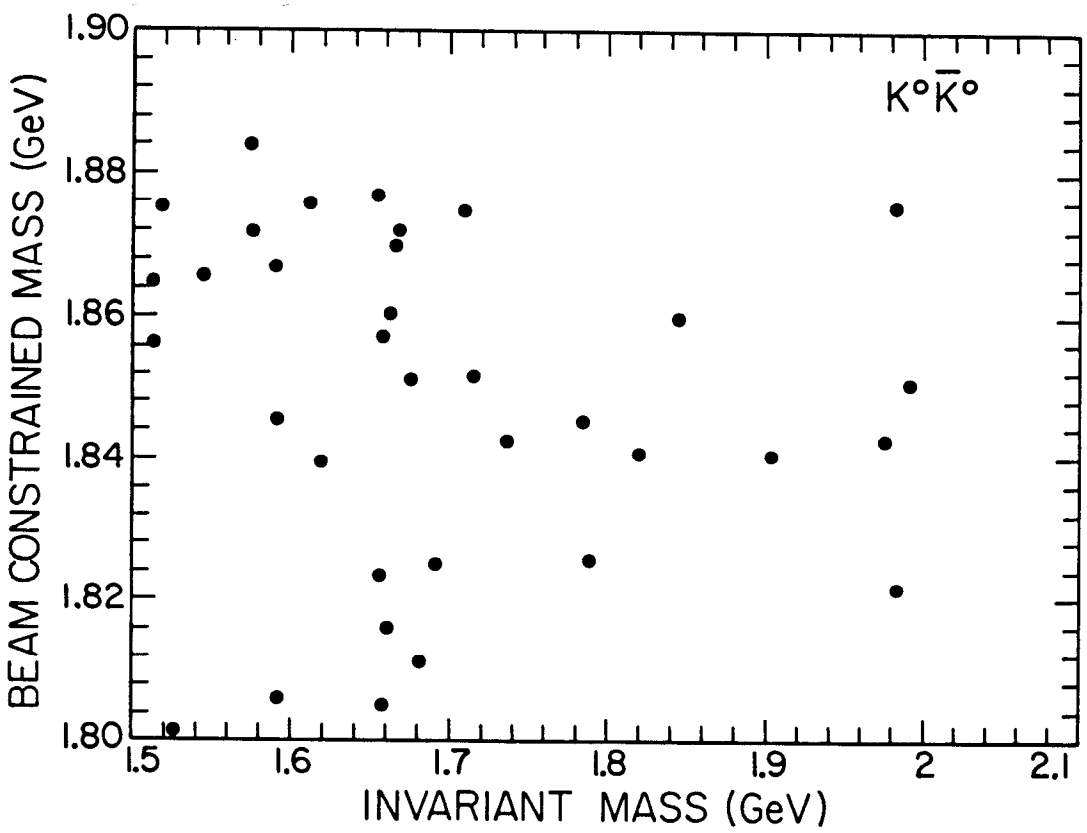
1.90
1.88
1.86
1.84
1.82
1.80
BEAM CONSTRAINED MASS (GeV)
K°K̄°
1.5
1.6
1.7
1.8
1.9
2
2.1
INVARIANT MASS (GeV)

Fig. 10

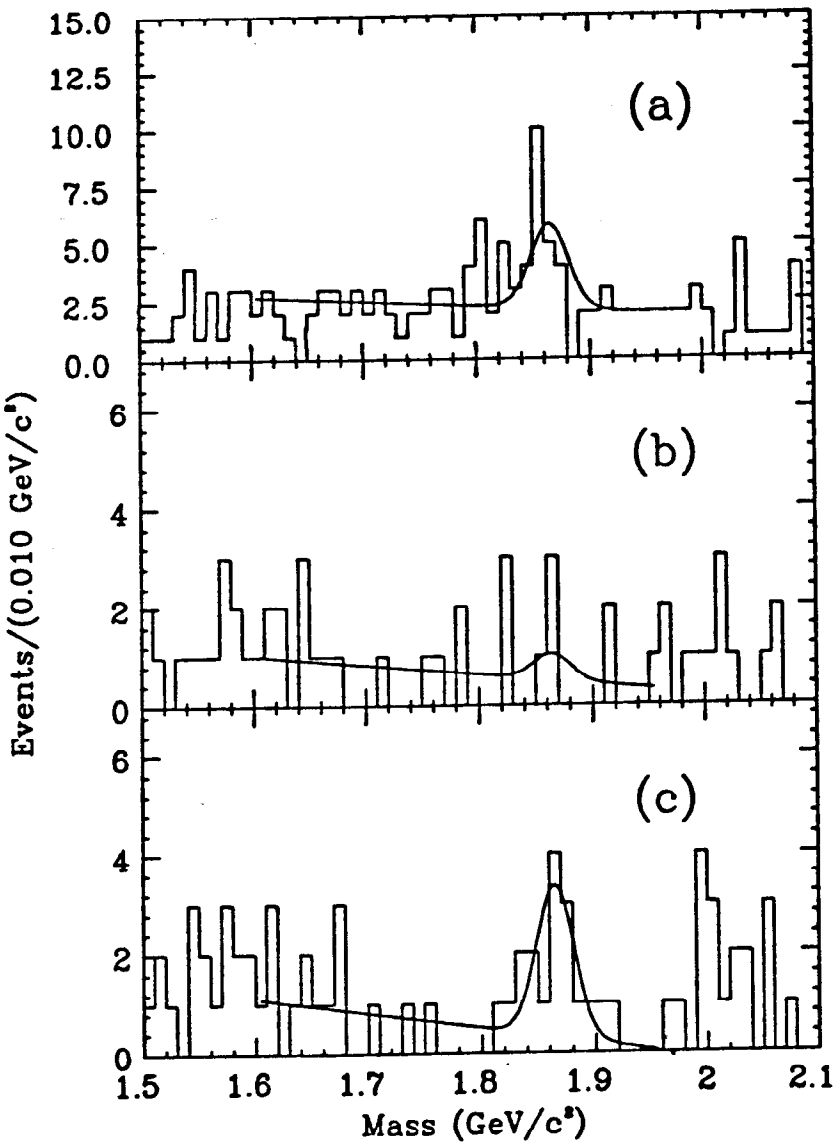
15.0
12.5
10.0
7.5
5.0
2.5
0.0
(a)
6
4
2
0
(b)
6
4
2
0
(c)
Events/(0.010 GeV/c²)
1.5
1.6
1.7
1.8
1.9
2
2.1
Mass (GeV/c²)

Fig. 11

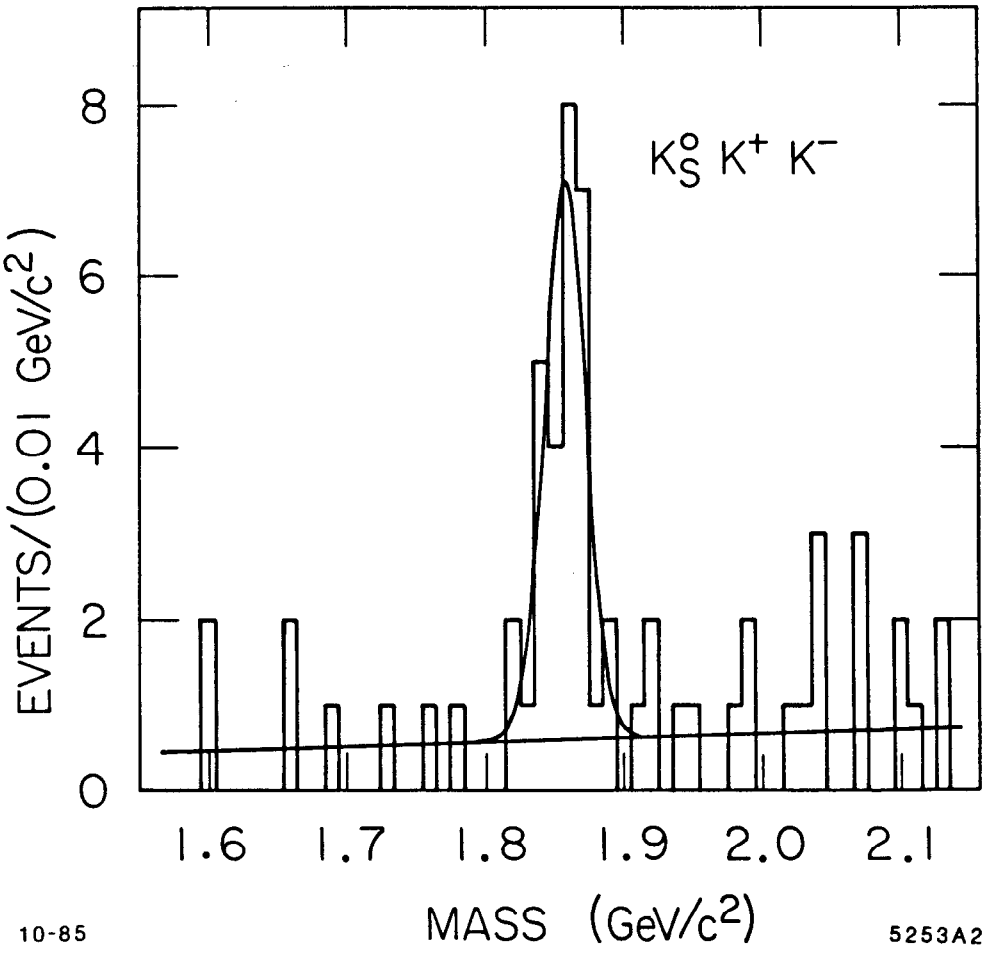
$K^0_S K^+ K^-$
EVENTS/(0.01 GeV/c²)
0
2
4
6
8
1.6
1.7
1.8
1.9
2.0
2.1
MASS (GeV/c²)
10-85
5253A2

Fig. 12

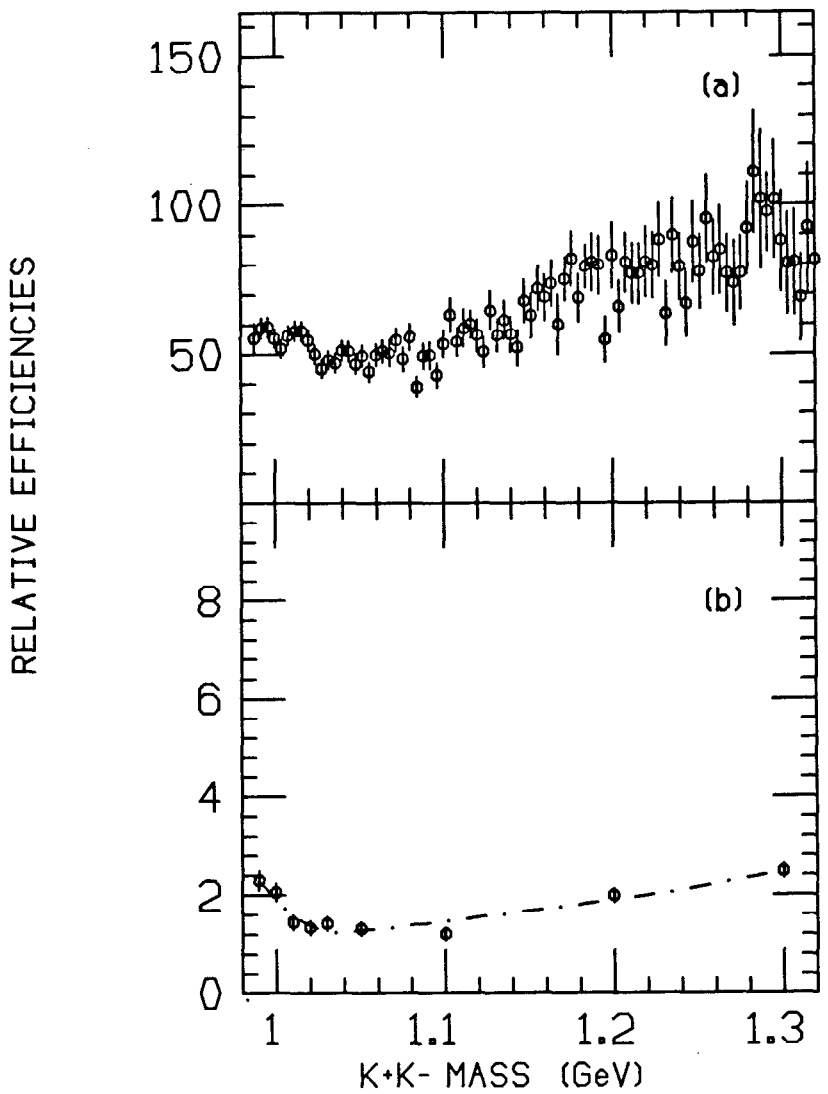
150
100
50
(a)
8
6
4
2
0
(b)
1
1.1
1.2
1.3
K+K- MASS (GeV)
RELATIVE EFFICIENCIES

Fig 13

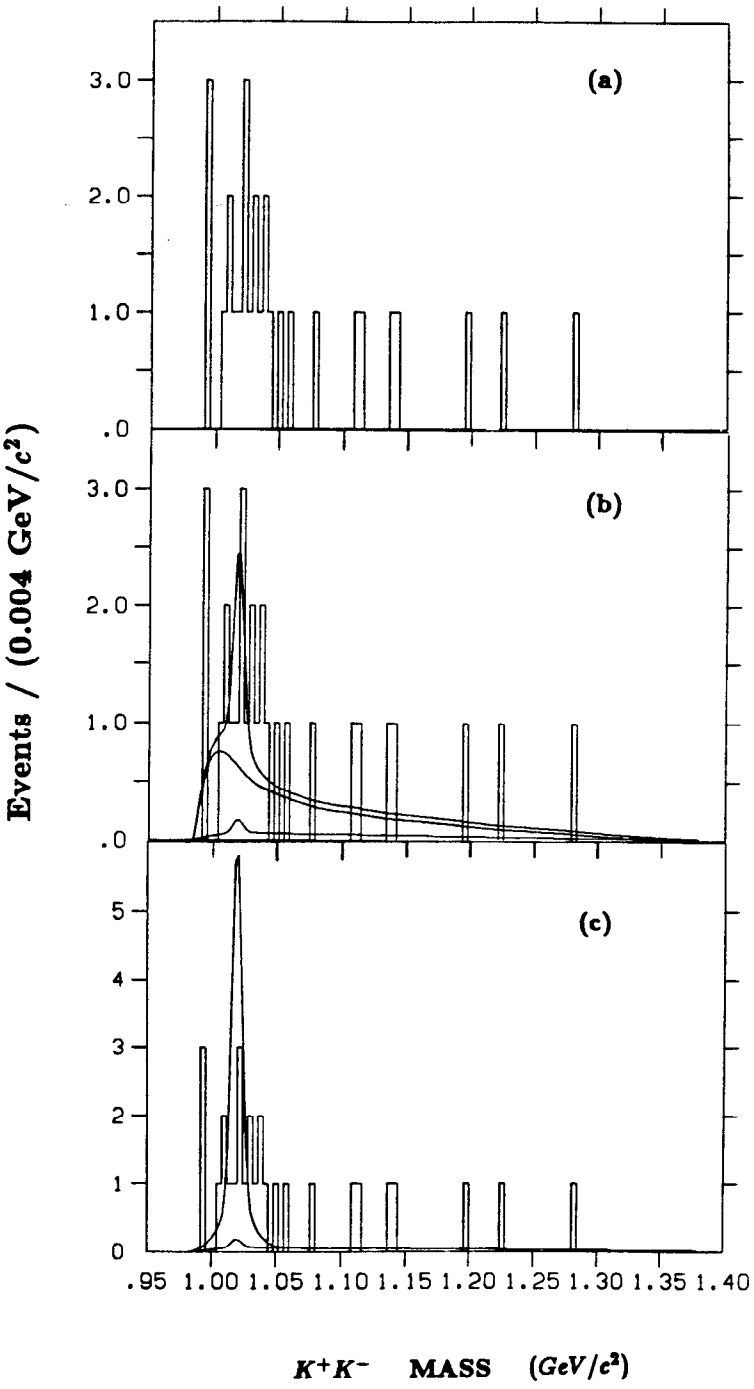
(a)
(b)
(c)
3.0
2.0
1.0
.0
5
4
3
2
1
0
.95 1.00 1.05 1.10 1.15 1.20 1.25 1.30 1.35 1.40
Events / (0.004 GeV/c^2)
K^+K^- MASS (GeV/c^2)

Fig. 14

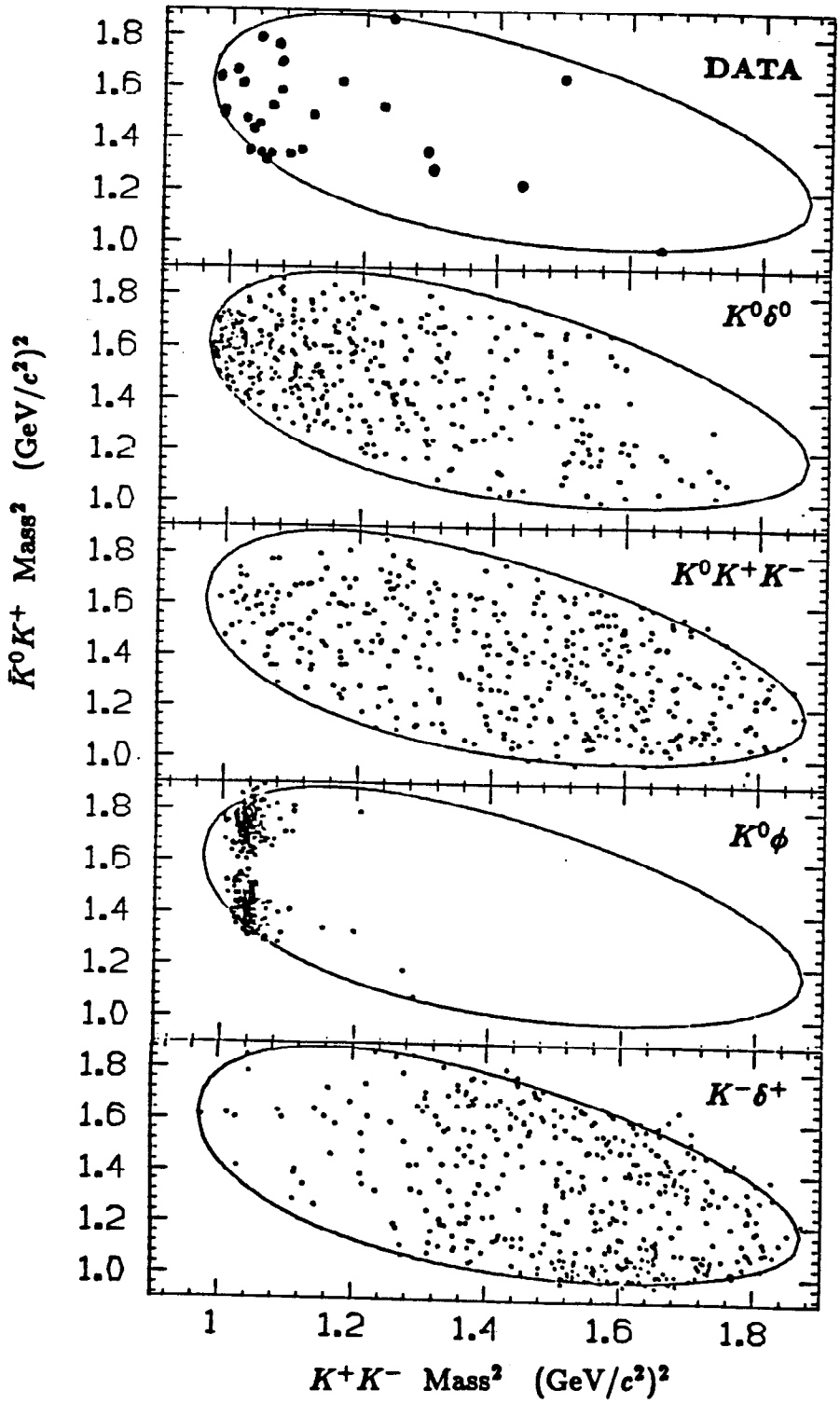
DATA
$K^0\delta^0$
$K^0K^+K^-$
$K^0\phi$
$K^-\delta^+$
K^0K^+ Mass^2 (GeV/c^2)^2
K^+K^- Mass^2 (GeV/c^2)^2
1.0
1.2
1.4
1.6
1.8
1

Fig 15

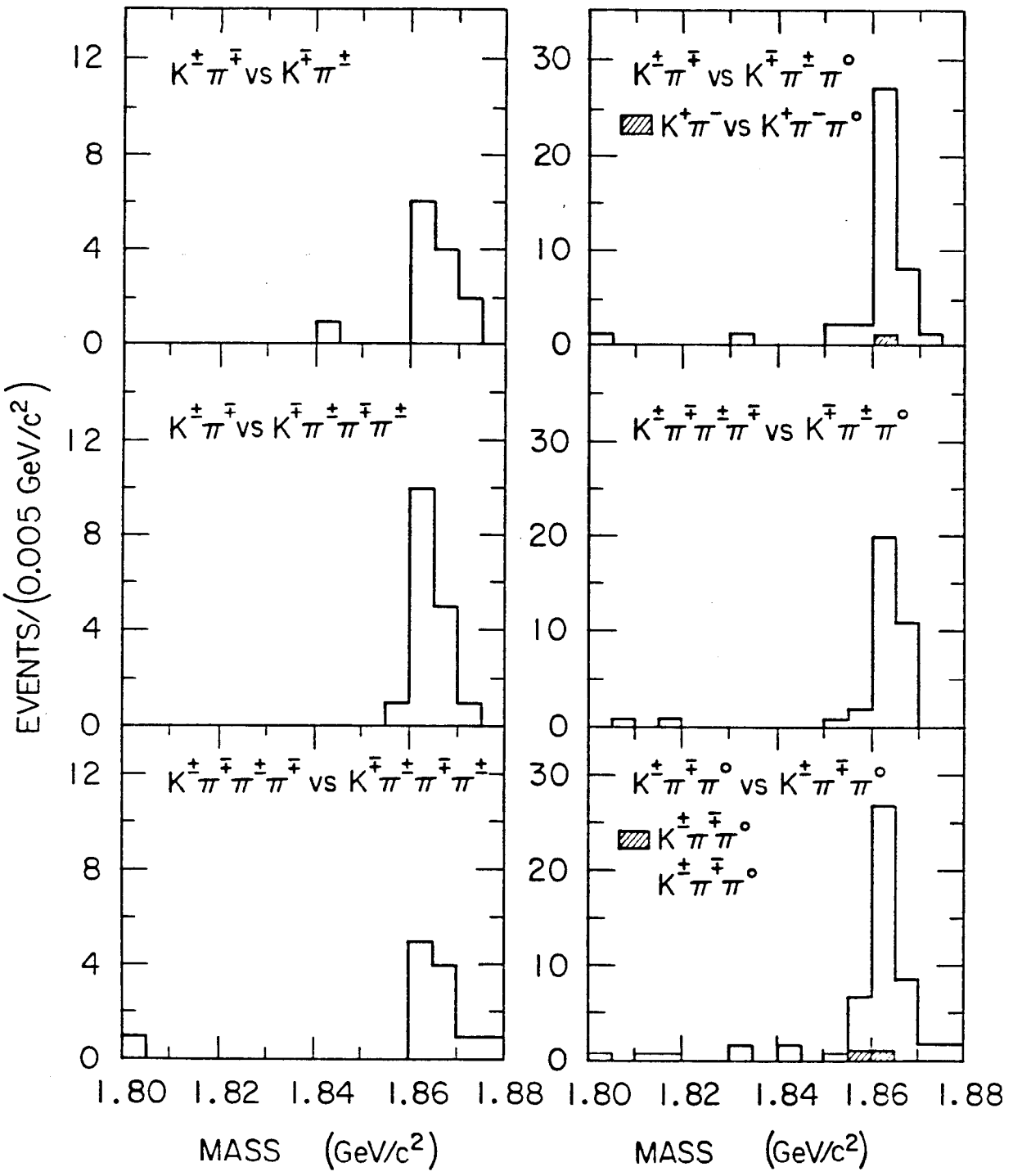
$K^{\pm}\pi^{\mp}$ vs $K^{\mp}\pi^{\pm}$
$K^{\pm}\pi^{\mp}$ vs $K^{\mp}\pi^{\pm}\pi^{\circ}$
$K^{+}\pi^{-}$ vs $K^{+}\pi^{-}\pi^{\circ}$
$K^{\pm}\pi^{\mp}\pi^{\pm}\pi^{\mp}$ vs $K^{\mp}\pi^{\pm}\pi^{\circ}$
$K^{\pm}\pi^{\mp}\pi^{\pm}\pi^{\mp}$ vs $K^{\mp}\pi^{\pm}\pi^{\mp}\pi^{\pm}$
$K^{\pm}\pi^{\mp}\pi^{\circ}$ vs $K^{\pm}\pi^{\mp}\pi^{\circ}$
$K^{\pm}\pi^{\mp}\pi^{\circ}$
$K^{\pm}\pi^{\mp}\pi^{\circ}$
EVENTS/(0.005 GeV/c^2)
MASS (GeV/c^2)
MASS (GeV/c^2)

Fig. 16

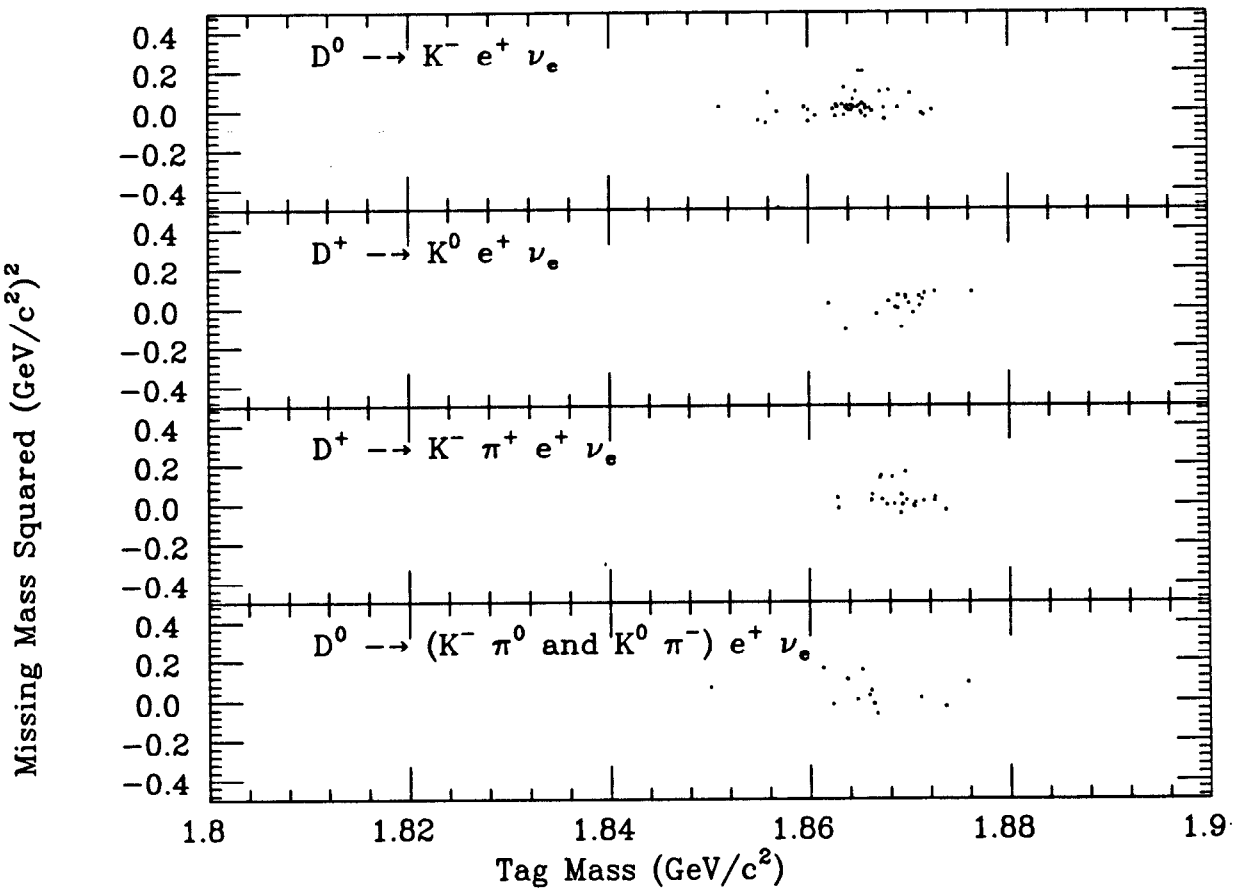
$D^0 \rightarrow K^- e^+ \nu_e$
$D^+ \rightarrow K^0 e^+ \nu_e$
$D^+ \rightarrow K^- \pi^+ e^+ \nu_e$
$D^0 \rightarrow (K^- \pi^0$ and $K^0 \pi^-) e^+ \nu_e$
Missing Mass Squared $(GeV/c^2)^2$
Tag Mass (GeV/c^2)
0.4
0.2
0.0
−0.2
−0.4
1.8
1.82
1.84
1.86
1.88
1.9

Fig. 17

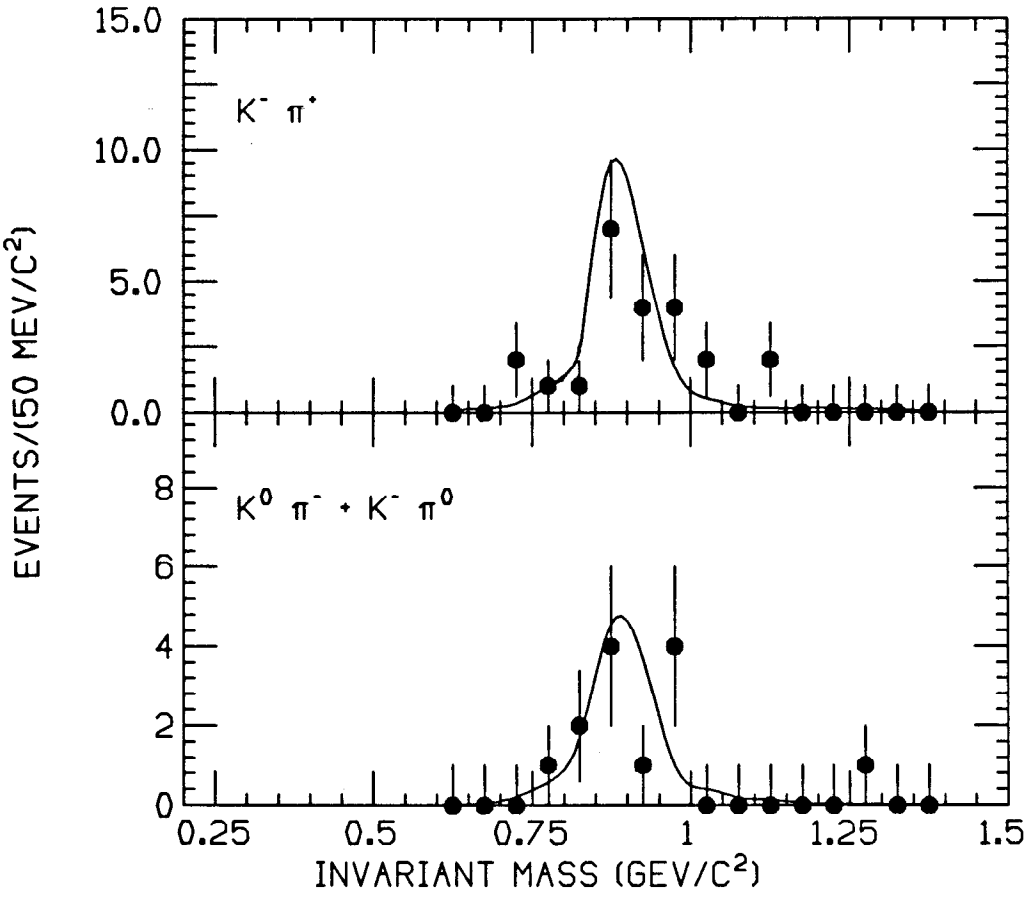
15.0
10.0
5.0
0.0
$K^- \pi^+$
8
6
4
2
0
$K^0 \pi^- + K^- \pi^0$
EVENTS/(50 MEV/C²)
0.25
0.5
0.75
1
1.25
1.5
INVARIANT MASS (GEV/C²)

Fig. 18

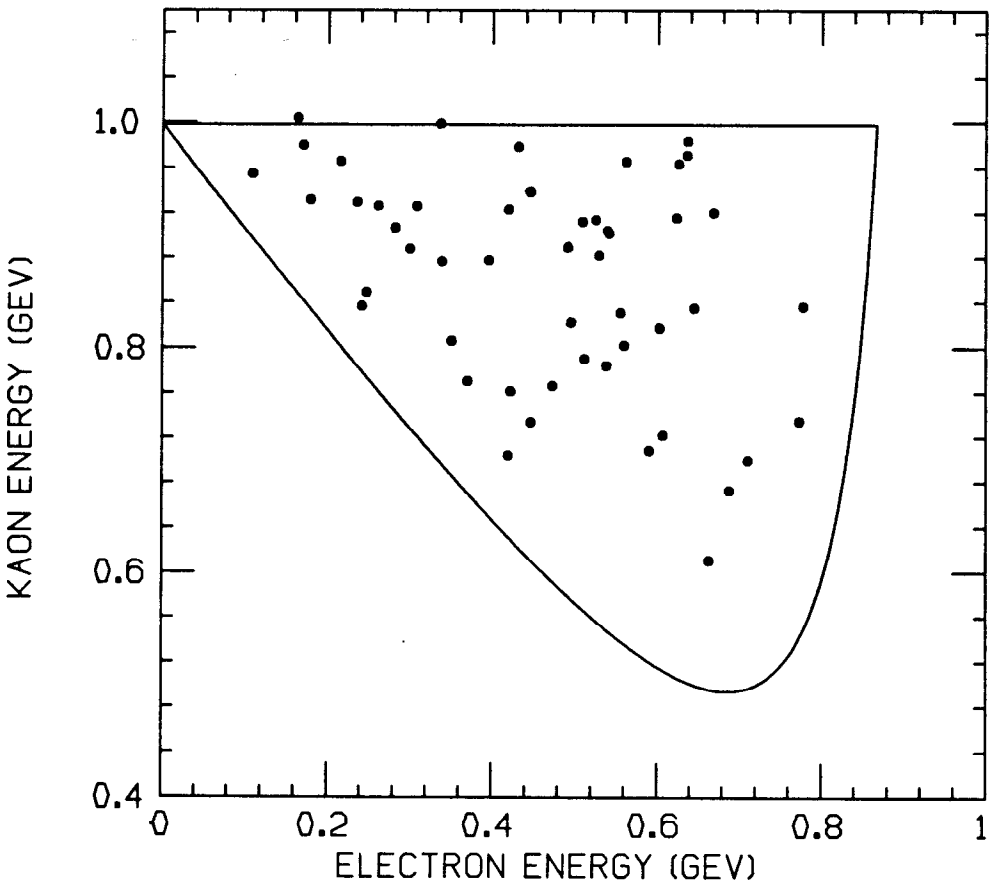

Fig. 19

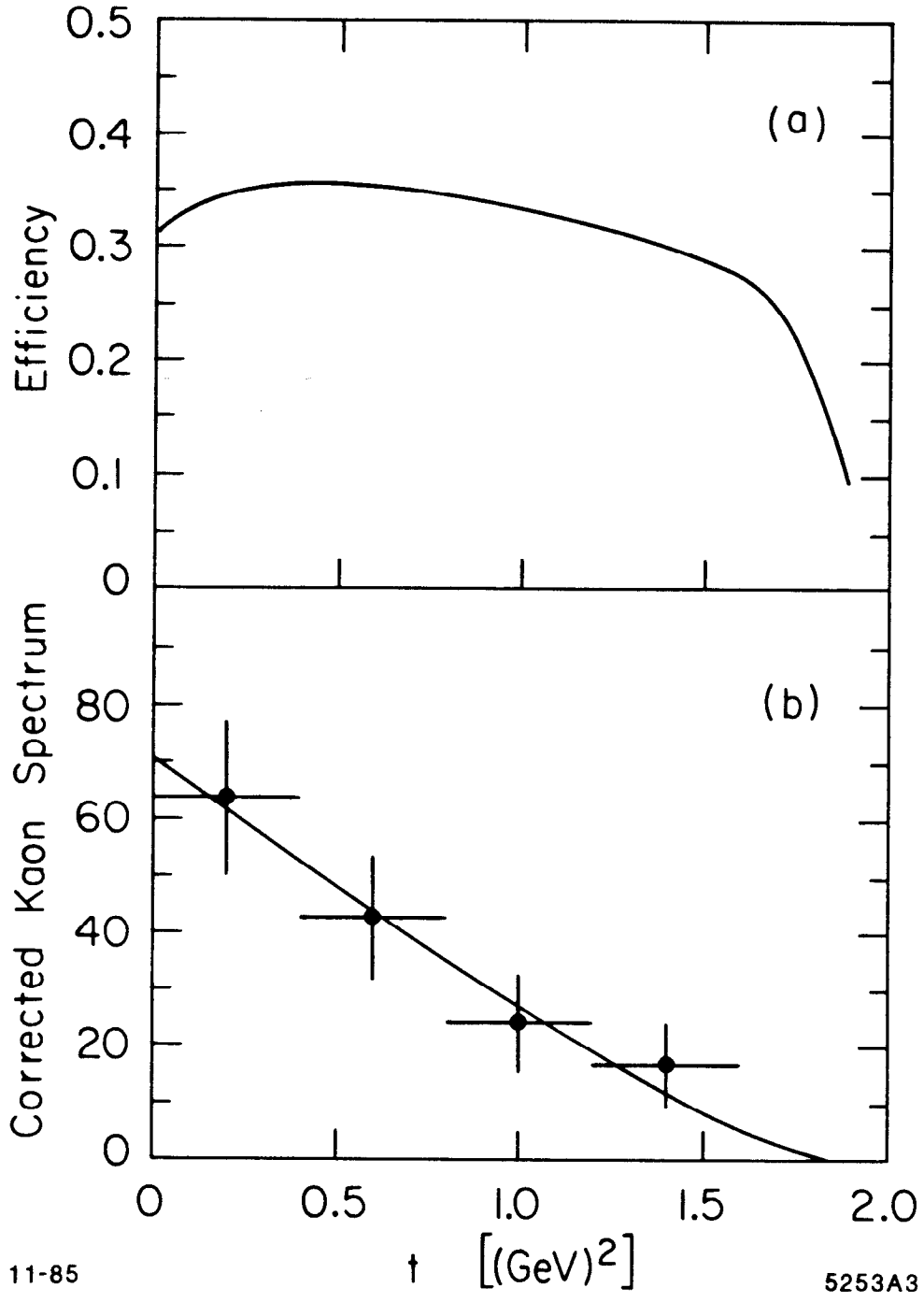
0.5
0.4
0.3
0.2
0.1
0
Efficiency
(a)
80
60
40
20
0
Corrected Kaon Spectrum
(b)
0
0.5
1.0
1.5
2.0
t [(GeV)2]
11-85
5253A3

Fig. 20